UNIVERSITY OF CALIFORNIA
UCO/LICK OBSERVATORY TECHNICAL REPORT
NO. 65

DESIGN, ANALYSIS, AND TESTING OF FIGURE CORRECTING CELLS FOR TWO 0.8-m LENSES

BRUCE BIGELOW

Santa Cruz, California
September 1992

Design, analysis, and testing of figure correcting cells for two 0.8-m lenses

Bruce C. Bigelow

University of California Observatories/Lick Observatory
University of California, Santa Cruz, CA 95064

UCO/Lick Observatory Technical Report No. 65

ABSTRACT

The design, analysis, and testing of two large, figure correcting lens cells are discussed. The two fused silica lenses, one biconvex and one meniscus, are approximately 800 mm (30 in.) in diameter. Both lenses were analyzed, using plate theory and finite element methods, and found to deform excessively under their own weight, regardless of mounting configuration. Consequently, cells were analyzed and designed, using the application of forces on the optics, which mechanically remove as much as 3 waves of astigmatism. The two lenses comprise the corrector for a large, all spherical, Schmidt-type camera system for the Keck Telescope High Resolution Echelle Spectrometer (HIRES). The camera sits on the Nasmyth platform of the telescope, with its optical axis down-looking at 10.3 degrees below horizontal. This paper describes the conceptual design of the cells, the finite element analysis of the lenses, detail design of the cells, and interferometric testing of the meniscus before and after installation in the cell.

1. CONCEPTUAL DESIGN OF THE CELLS

Preliminary analysis of the corrector lenses indicated that due to the large diameters and thin cross-sections, the lenses (see dwg H0148) would deform unacceptably under their own weight. The optical design[1] and mechanical stiffness of the lenses could have been improved by thickening the elements, and but cost and manufacturing limitations at Corning precluded that option. When faced with the fixed lens geometry and unacceptable self-load deformations, the Principal Investigator for HIRES, Dr. Steven S. Vogt, said "Well, just bend them back into shape".

Figure correction of mirrors by passive and active means have been well documented and successfully realized in a variety of cases[2,3,4]. However, a review of the literature for optomechanics, and lens mounting in particular, did not turn up any mention of passive nor active figure correction for lenses. So the challenge became the development of a support and figure correcting scheme which would "reform" the lenses back into acceptable figures. The time and money budgeted for completing the optical support systems precluded a long and involved research and development exercise. Consequently, the supports would have to be fairly simple, relatively inexpensive, and reasonable to manufacture and assemble. A previous paper discussed the initial finite element analyses of the lenses, and a more complicated plan of attack for static figure correction[5]. The earlier work was completed without a good understanding of the required clear apertures, and consequently did not take advantage of the areas on the lenses which were outside the required aperture. In fact, the echelle and cross-dispersed beam is roughly rectangular, with the long axis rotated about 8° from vertical. The clear aperture only uses about 60% of the total aperture of the lenses. Once the beam profile was known, it was clear that the forces could be applied closer to the center of the lenses, and that two force points would be sufficient. With a conceptual layout of the support and constraining points, a second round of finite element analysis was undertaken to determine the optimum locations and values for the reforming forces.

2. FINITE ELEMENT ANALYSES OF THE LENSES

The initial finite element analyses for the lenses were described in the previous paper. The same general input routine was used again, with an added sub-routine for applying the reforming forces. The ANSYS® finite element models typically used about 1450 nodes, 1050 3–D solid elements, and 4200 degrees of freedom. More than thirty trials were completed for each lens, manually varying the force or location with each run. Given enough computing power, this process could be automated for a more complete optimization. Still, a variety of solutions showing a $\lambda/4$ P-V optical path difference (OPD) were found, and the location requiring the least force was used in each case (see ANSYS input files in Appendixes A and B). Figure 1 shows a typical finite element model of the meniscus lens, showing the defining points, symmetry boundary conditions, and the locations of the reforming forces. Figures 2 and 3 show the finite element predictions for deformation of the meniscus lens before and after the application of the forces. Figures 4 and 5 show the same plots for

the biconvex lens. Note that although the overall P-V deformations are more than $\lambda/4$, the clear apertures (outlined) are $\lambda/4$ P-V. It is important to note that the reforming forces induce stresses in the fused silica lenses, and consequently contribute birefringence effects to the optical path length errors. However, because the stresses never exceeded 50 psi, well below the accepted 500 psi limit for birefringence[6], the OPD errors were considered negligible.

3. DETAIL DESIGN OF THE CELLS

As mentioned before, a variety of considerations drove the design process for the corrector cells. The support of the optical system was part of a fixed price/schedule project, which precluded extensive (and expensive) design and development options. The corrector lenses would ultimately be anti-reflection coated using a Sol-Gel process, developed and applied at Lawrence Livermore National Lab for the Nova Laser Program. This coating was expected to be stripped and reapplied occasionally, which required that the lenses be completely and readily separable from their cells, and precluded "potting", or elastomeric mounting. The cells would be manufactured in the Lick Observatory Instrument Labs, which required that relatively benign materials and conventional fabricating process be used. As usual, cell weight would be minimized to reduce cost and gain "trickle down" weight savings for the instrument. Light weight would also be a benefit for assembly and handling. Although the final installed environment would be stable in both temperature and humidity (Mauna Kea, Hawaii: 13,796 ft, +/-2°F/day), corrosion resistant materials and surface treatments would be used throughout. Detail design of the radial supports, axial supports, force application assemblies, and cells will be discussed in that order.

3.1 Radial Supports

The justifications for the basic design of the radial supports is discussed in the previous paper. To summarize, the radial support contacts are split twice in the theta direction, and twice again in the z-direction (see detail A, dwg H5324). The balance beams operate in both directions in order to reduce the bearing stresses in the optic. Two sets of two radial supports were found to provide comfortably low contact stress and minimized the deformation of the lenses. Stainless-steel flex pivots were designed to minimize the axial forces transferred to the optic, while allowing minor focus adjustments without lifting the lens off of the support. The flex pivots reduce (but do not eliminate) the risk of axially overconstraining the lens. The Delrin contact pads are mounted to the second flex pivot, in this case a machined feature, to divide the load across the lens center of gravity, again reducing stress and avoiding local deformation of the figure. A single threaded post at the top of the cell constrains the lens in the cell during handling or unexpected accelerations.

3.2 Axial Supports

The axial supports provide two functions in the correcting lens cells. First, the axial constraints define the location of the optical surface, and provide a way to align the optical axis of the part. Second, the axial contacts provide a location for the force points to react against. So in addition to locating the lens, the axial constraints help to reform the figure. The design of the defining points and backside constraints are identical for both lens cells. The defining surface axial contacts are composed of extra-fine threaded stainless steel posts, with commercial swivel-feet and Delrin caps to follow and protect the surface of the lens (see dwg H5328). The backside axial constraints are primarily "earthquake clips", to prevent the lens from falling out of its cell during handling or unexpected accelerations. The backside contacts are also extra-fine threaded stainless steel shafts, with spherical Delrin tips (see dwg H5328). In the case of the meniscus, the forces applied to correct the figure actually transfer the lower pair of axial loads to the back of the lens, causing the backside constraints to become the defining points.

3.3 Force application assemblies

The force application assemblies (force points) provide a means for applying an adjustable, known force on the optics. The force point consists of a stainless steel shaft, a swivel-foot/Delrin cap, a threaded brass adjusting body, a spring, and a stainless steel end cap (see dwg H5328). The springs are standard commercial parts that were calibrated for use in the force points. Although the forces applied to the two lenses are different by a factor of two, the force points are identical except for the stiffness of the springs. The length and spring constants for the springs were selected so that both would require about 0.5" of compression to apply the desired force (11.5 lbs for the meniscus, 6.0 lbs. for the biconvex lens). The springs can be compressed from each end, either by tightening the end cap, or by tightening the brass adjusting body. The two adjustments allow for very fine tuning of the force applied, and allow the force point to compensate for axial adjustments of the lens.

3.4 Lens cells

The cells house the lenses and provide a base for attaching the defining and forcing hardware. The housing is composed of two stiffened face plates which are screwed to a ring weldment. This construction is relatively light weight and allows the cell to be dismantled for installing or removing the lens. The remainder of the cell includes a door for dust protection, and a hoisting ring for handling. Drawings H5324 and H5349 show the complete lens and cell assemblies. For reference, the corrector lenses both weigh about 120 lbs., the meniscus and biconvex cells weigh 130 lbs. and 110 lbs. respectively.

4. LENS TESTING

The preliminary optical specification for the corrector lenses was to achieve a P-V OPD of $\lambda/4$ over the specified clear apertures. This is probably the easiest value to work towards during finite element analysis as well as for figuring in the Optical Lab. However, later analysis of the optical system indicated that local slope errors were much more important than the overall P-V figure on a given surface.

4.1 Biconvex lens testing

Due to convex surfaces and long radii of curvature, it was not practical to perform interferometric testing on the biconvex lens. Instead, all testing of the biconvex lens was completed using 10" diameter test plates. Although the test plates cannot qualify the peak-to-valley specification for the full aperture, they do give an excellent representation of local slope errors. Based on test plate measurements, the biconvex lens was found to be better than $\lambda/4$ over any given 10" aperture. The following section will focus entirely on the testing of the concave surface of the meniscus lens, which was the only surface readily tested with the interferometer.

4.2 Meniscus lens testing

The meniscus lens was tested in two different positions to confirm the results of the finite element analysis and to verify that the figure as polished was still acceptable after installation and figure correction in the cell. In each case, interferograms were taken and the Wyco WISP® program was used for fringe analysis. Zenith-pointing testing was conducted with the lens mounted on a foam-lined support which was in turn carried on a large vibration isolation structure (see dwg H5811). Interferograms were taken for several rotations of the lens relative to the foam support. The figures were consistent at about 1.5λ P-V, mostly astigmatism, and 0.25λ RMS (see figures 6,7,8).

The next set of tests were run in the final, tilted orientation. The lens cell and interferometer were assembled on a Newport Research Series vibration isolation table down-looking (see dwg H5826). The first set of tests were to establish the deformed figure without any correcting forces applied. The finite element model predicted about 2 waves of deformation across the full aperture (figure 2). The measured figure was a little more than 4 waves P-V (figures 9,10,11), roughly twice the expected amount. By carefully maintaining a fiducial location on the lens, it was possible to subtract the known figure on the lens from the figure seen in the cell (figures 12,13). However, this still left a discrepancy of about 1.5 wave between the predicted and measured values. No clear explanation for the difference has been determined yet, although errors in the FEA model, errors in the design and/or assembly of the cell, and errors on the lens have all been considered.

The third set of tests involved applying the correcting forces and taking more interferograms. One of the goals at this stage was to determine if the predicted correcting forces were in fact the optimum. Tests were run at 1 lb. intervals above and below the predicted optimum of 11.5 lbs. The sense of the deformation was seen to switch between 10.5 lbs. and 12.5 lbs., suggesting that 11.5 lbs. really was the best value, over the range tested. By applying the optimum 11.5 lb. force at each location, the overall figure improved from 4.34 waves to 1.47 waves, a reduction of almost 3 waves of astigmatism (figures 14,15,16). In this case, removing the lens figure from the deformed figure did not show any significant improvement in the P-V OPD. The 1.47λ P-V was still much worse than the 0.3λ P-V (see figure 3) prediction from the finite element model, but nevertheless was a dramatic improvement realized by a rather simple mechanical correction. The FEA predictions and interferograms do agree quite well on the topography of the deformed (astigmatic) shape, but the FEA model underestimates the amplitude of the deformation by almost 5 times. Finite element models are typically reliable to 10-20%, not 500%, so there is clearly a problem somewhere. Possible contributors include errors in the FEA model, the figure on the lens, errors in the location or assembly of the lens in its cell, or other testing error.

The last interferogram shows the figure over the required clear aperture (figures 17,18,19). For this area, the P-V OPD is 0.68λ and 0.10 RMS. Again, the P-V number is worse than predicted, but the RMS value is actually quite good. The fringe analysis program indicated that the worst slope error was 2.1λ/14.15" (the pupil radius), for a maximum slope of 3.7×10^{-6} radians. The slope error can then be multiplied by the focal length of the lens to determine the worst case typical ray deviation at the focal plane. In this case, the maximum deviation was 1.4μm and the RMS image diameter was 1.2μm. The diffraction limited image diameter was 1.64μm, suggesting that the concave surface was essentially diffraction limited. This conclusion was also indicated by the 0.66 Strehl ratio calculated by WISP (figure 18).

5. CONCLUSIONS

Two novel figure-correcting lens cells were analyzed, designed and tested. Finite element models were successfully used to predict the optimum forces and locations for applying corrections to the lenses. Although the FEA predictions seriously underestimated the amplitude of the deformations, the models closely matched the measured topography of the figures. This result suggests that there is room for improvement in the modeling process, although it is not entirely clear whether the disagreement lies in the FEA, the design or assembly of the cell, or the testing methods. Although much work remains to be done in improving the accuracy of the figure correcting cell, the concept has been tested and proven able to remove as much as 3 waves of elastic deformation.

6. ACKNOWLEDGMENTS

This work was performed as a part of design and development of the Keck Telescope High Resolution Echelle Spectrometer, and was funded by the California Association for Research in Astronomy (CARA). Dr. Steven S. Vogt was Principle Investigator, responsible for the overall conceptual design of the spectrograph. Dr. Harland W. Epps was responsible for the unique optical design of the camera system. David Hilyard ground and figured the optics, and performed the extensive testing and fringe analysis. Many people from the Lick Observatory Instrument Lab participated in the fabrication and assembly of the lens correcting cells, with special thanks to, Jeffrey P. Lewis, M. Terrance Pfister, and James A. Ward. Jack Osborne provided technical support and encouragement throughout the design, analysis, and fabrication of the cells. Carol Osborne did the hard part, drafting and detailing 300 E-size sheets of drawings for the optical cells, structures, and test fixtures.

7. REFERENCES

1. H. W. Epps and S. S. Vogt, Applied Optics, in press.

2. T. S. Mast, J. E. Nelson, "The fabrication of Large Optical Surfaces Using a Combination of Polishing and Mirror Bending", Proceedings of the SPIE conference on Advanced Technology Optical Telescopes IV, L. D. Barr Ed., pp. 671– 681, Vol 1236, part 2, Tuscon, 1990

3. P. Y. Bely, D. A. Salmon, P. L. Wizinowich and A. Tournaire, "Bending the CFHT Cassegrain Secondary for Optical Figure Improvement", Proceedings of the SPIE, pp. 253, Vol. 444, London, 1983

4. L. Noethe, F. Franza, P. Giordano, R. N. Wilson, and M. Tarenghi, "Active Optics: From the Test Set up to the NTT in the Observatory", Proceedings of the SPIE Conference on Active Telescope Systems, pp. 314, Vol. 1114, Orlando, 1989.

5. B. C. Bigelow, "Finite Element Analysis of Large Lenses for the Keck Telescope High Resolution Echelle Spectrograph", Lick Technical Report #59 and Proceedings of the SPIE Conference on Analysis of Optical Structures, D. C. O'Shea Ed., pp 15, Vol. 1532, San Diego, 1991

6. P. R. Yoder, Opto-Mechanical Systems Design, Chap. 4, Marcel Dekker, Inc., New York, 1986

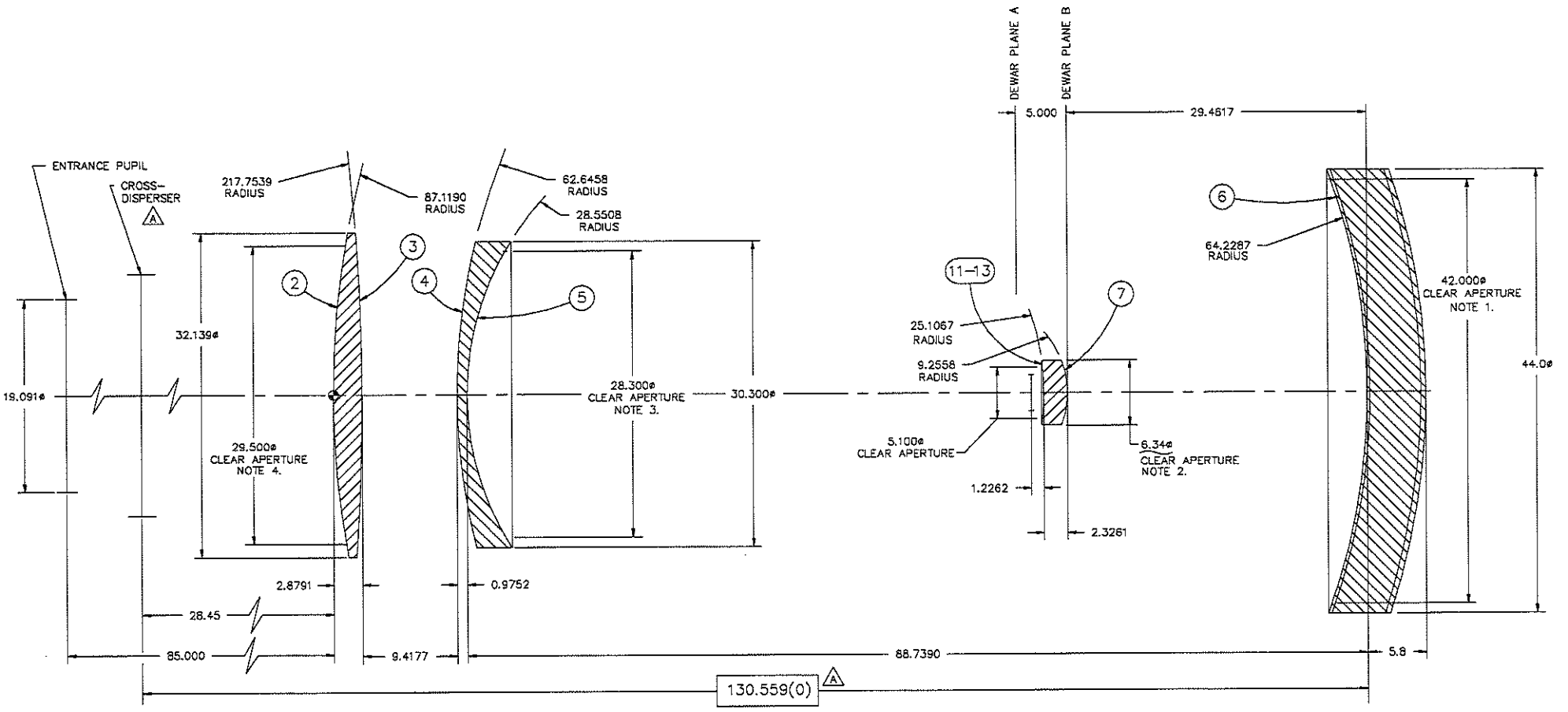

(-1) EPPS DESIGN #4052 (6/3/92)

FINAL "AS-BUILT" PRESCRIPTION
USE WITH R=65.0" CONVEX TEK CCD
T = 0°C
THIS DRAWING REPLACES H0135, SUPER-DUPER II
WHICH WAS EPPS DESIGN #7465 (11/15/90)
THE FLAT FIELD VERSION #4753 IS DRAWING H0149.

NOTES:
1. 37.603ø CLEAR APERTURE FOR THIS CCD.
SEE H5400-H5405, H5415, H0144 FOR DETAILS
2. 6.34ø C.A. FROM 6.44ø BLANK
SEE H7181 FOR LENS DETAIL
3. 25.90ø C.A.
SEE H0136, H0142, H0145, H0147
4. 27.13ø C.A.
SEE H0136, H0141, H0146

A | 8 11 92 | J.G. | ADD DIMENSION TO CROSS-DISPERSER

KECK/HIRES
SUPER-DUPER CAMERA III
AS-BUILT "CURVED FIELD"
H.EPPSø 3 92
J.G. 4 3 92
H0148.A

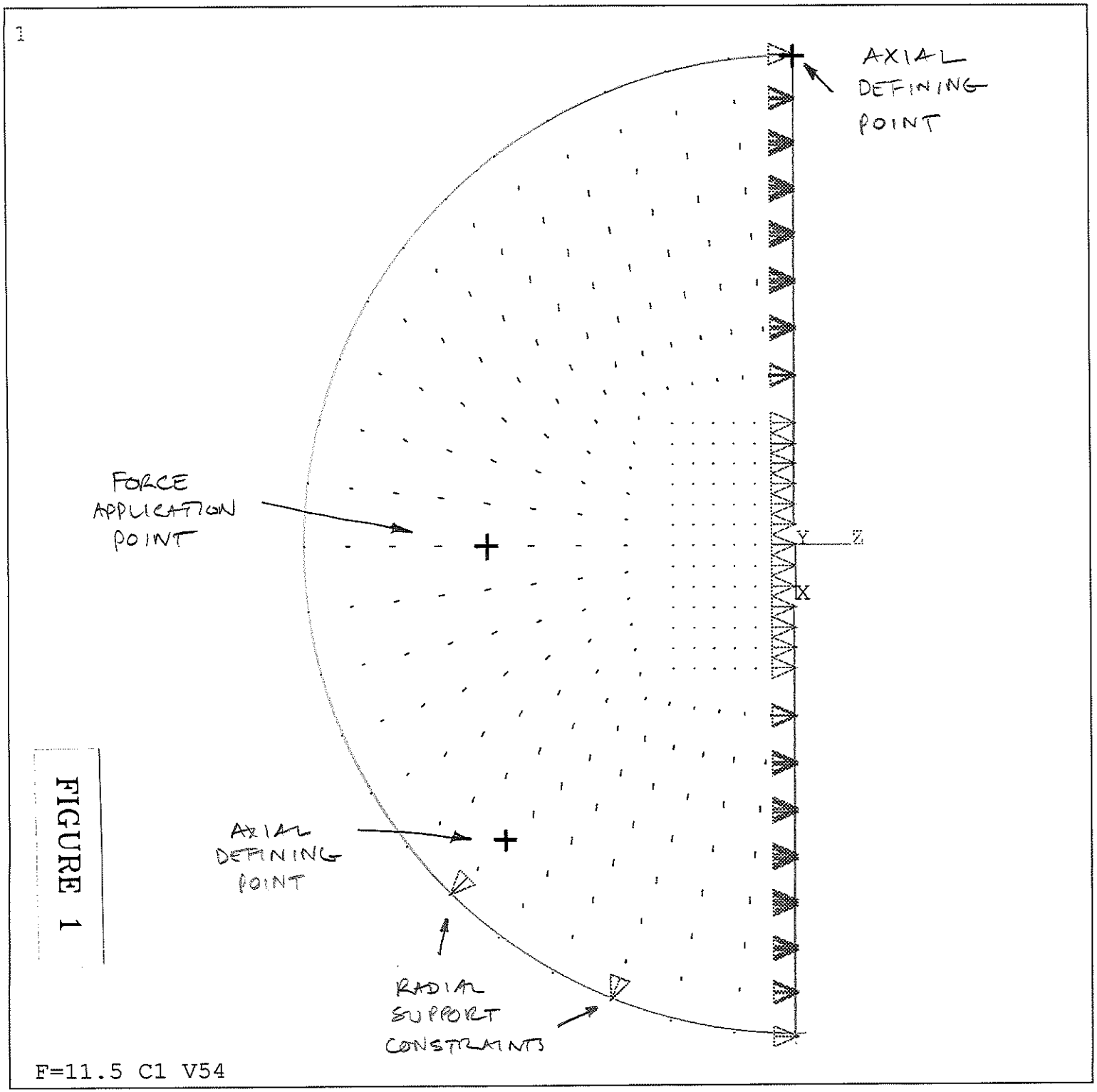

FIGURE 1

ANSYS 4.4A
JUL 22 1992
15:37:25
PLOT NO. 1
PREP7 NODES
TDIS
FORC

YV =-1
DIST=16.678
YF =1.68
ZF =-7.581
VUP =-X

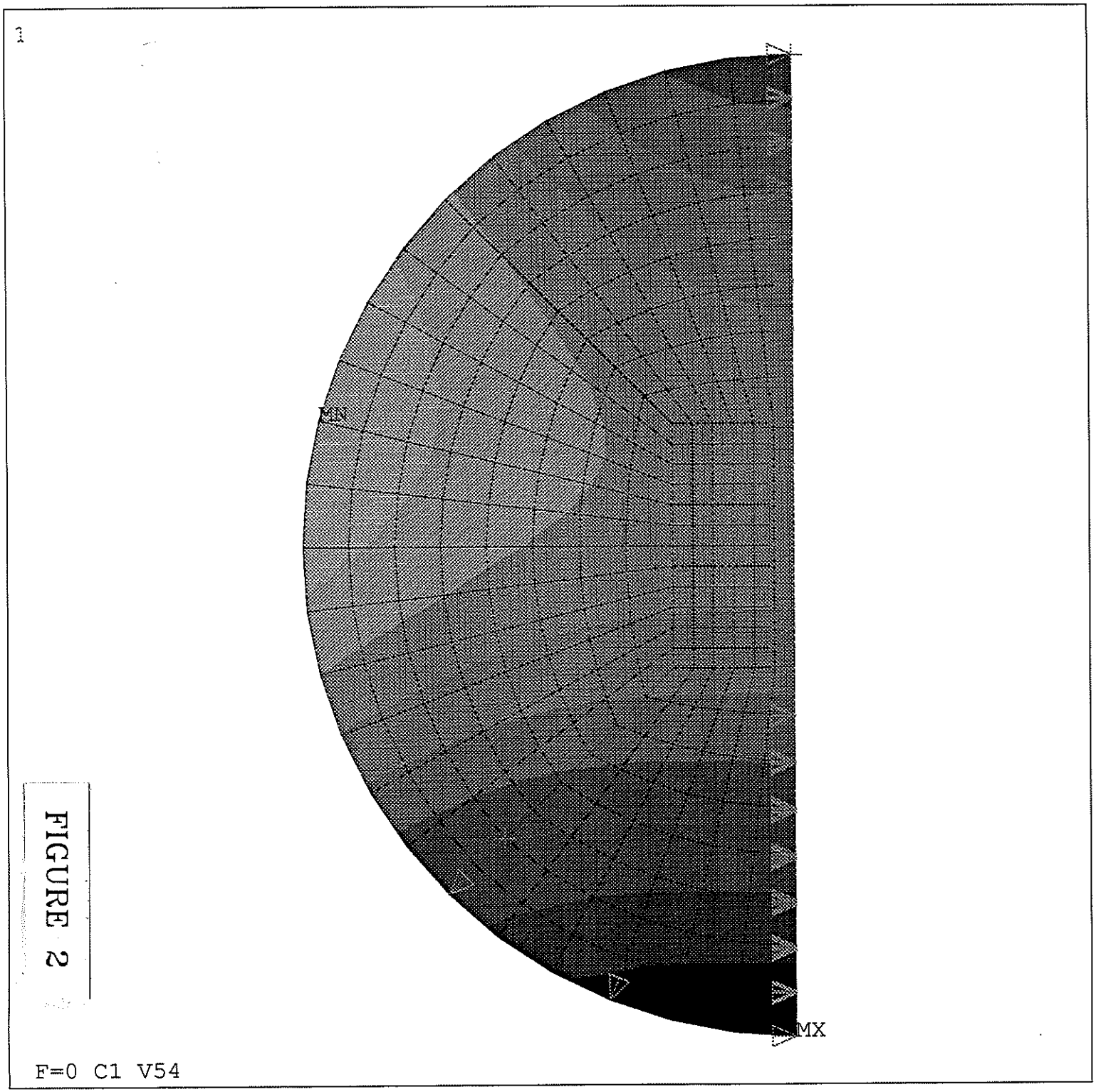
ANSYS 4.4A
JUL 22 1992
16:10:57
PLOT NO. 1
POST1 STRESS
STEP=2
ITER=1
UY
D GLOBAL
SMN =-0.358E-04
SMX =0.182E-04
TDIS
YV =-1
DIST=16.678
YF =1.68
ZF =-7.581
VUP =-X
FACE HIDDEN
-0.358E-04
-0.298E-04
-0.238E-04
-0.178E-04
-0.118E-04
-0.580E-05
0.194E-06
0.619E-05
0.122E-04
0.182E-04
MN
MX
F=0 C1 V54

FIGURE 2

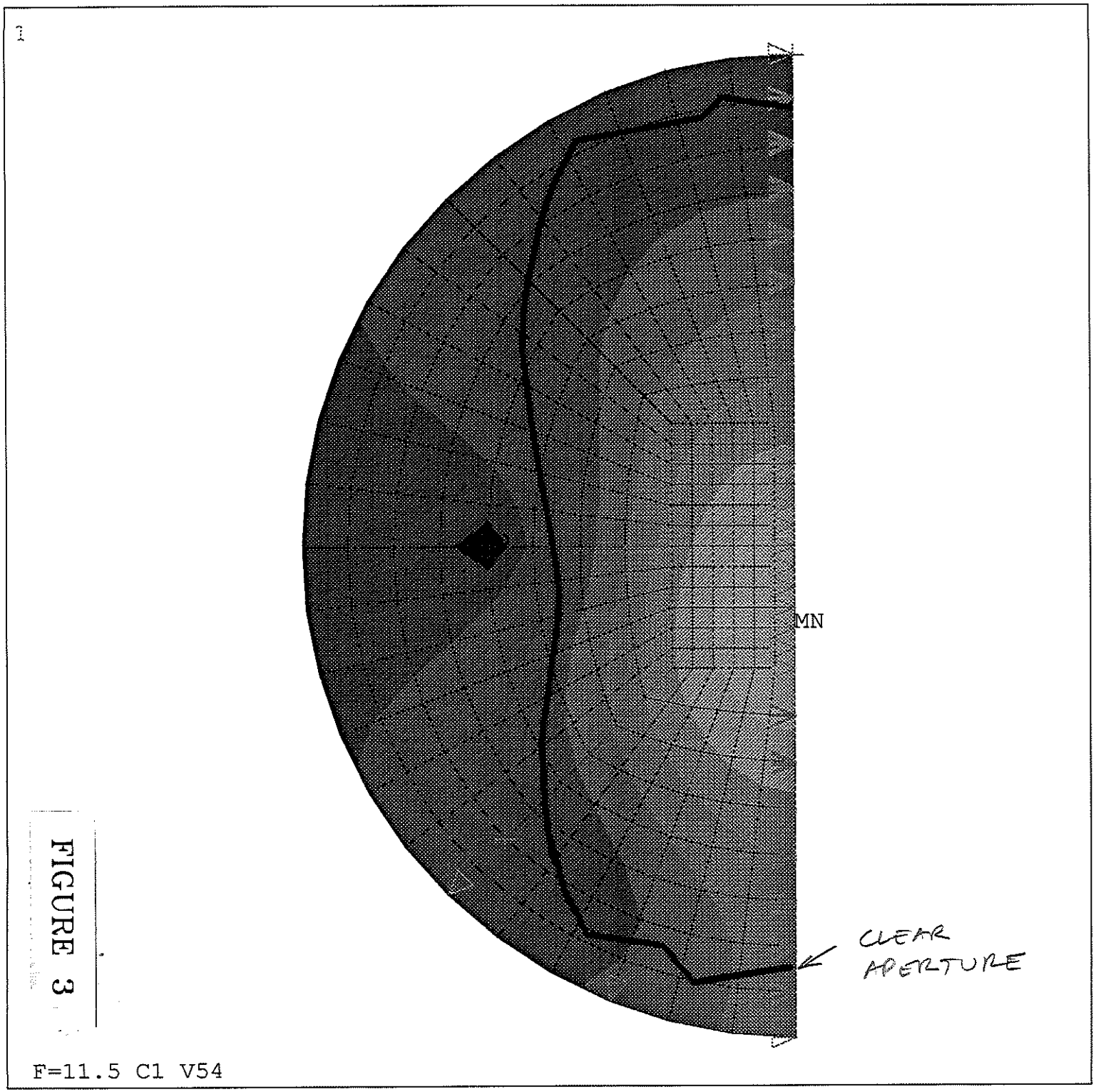
1
ANSYS 4.4A
JUL 22 1992
15:39:08
PLOT NO. 1
POST1 STRESS
STEP=3
ITER=1
UY
D GLOBAL
SMN =-0.558E-05
SMX =0.247E-05
TDIS
YV =-1
DIST=16.678
YF =1.68
ZF =-7.581
VUP =-X
FACE HIDDEN
-0.558E-05
-0.469E-05
-0.379E-05
-0.290E-05
-0.200E-05
-0.111E-05
-0.216E-06
0.678E-06
0.157E-05
0.247E-05
MN
CLEAR APERTURE
F=11.5 C1 V54

FIGURE 3

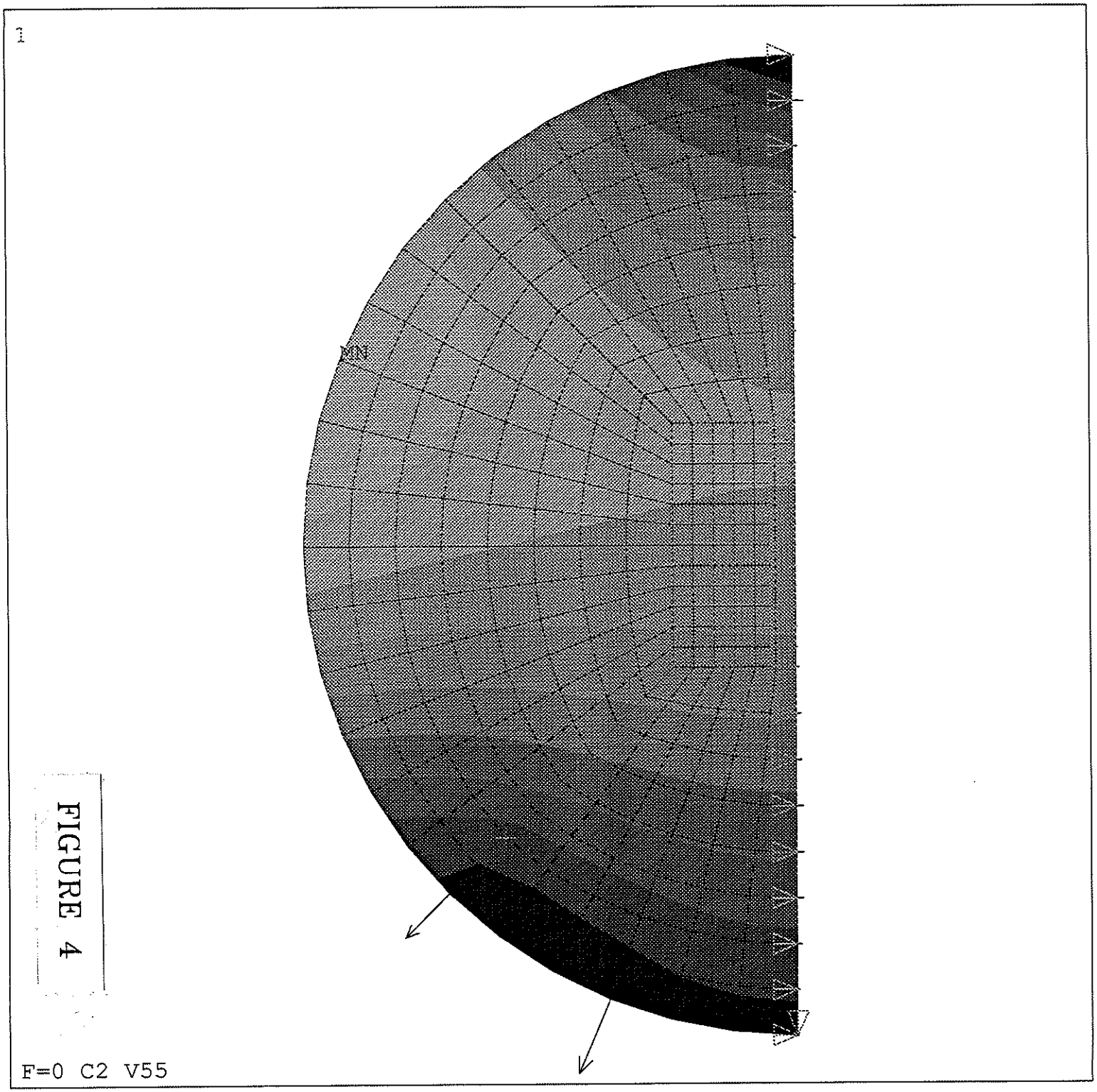
1
MN
ANSYS 4.4A
AUG 18 1992
13:48:02
PLOT NO. 2
POST1 STRESS
STEP=2
ITER=1
UY
D GLOBAL
SMN =-0.298E-04
SMX =0.590E-05
TDIS
FORC
YV =-1
DIST=17.677
YF =-1.437
ZF =-8.035
VUP =-X
FACE HIDDEN
-0.298E-04
-0.258E-04
-0.219E-04
-0.179E-04
-0.139E-04
-0.997E-05
-0.600E-05
-0.203E-05
0.193E-05
0.590E-05
F=0 C2 V55

FIGURE 4

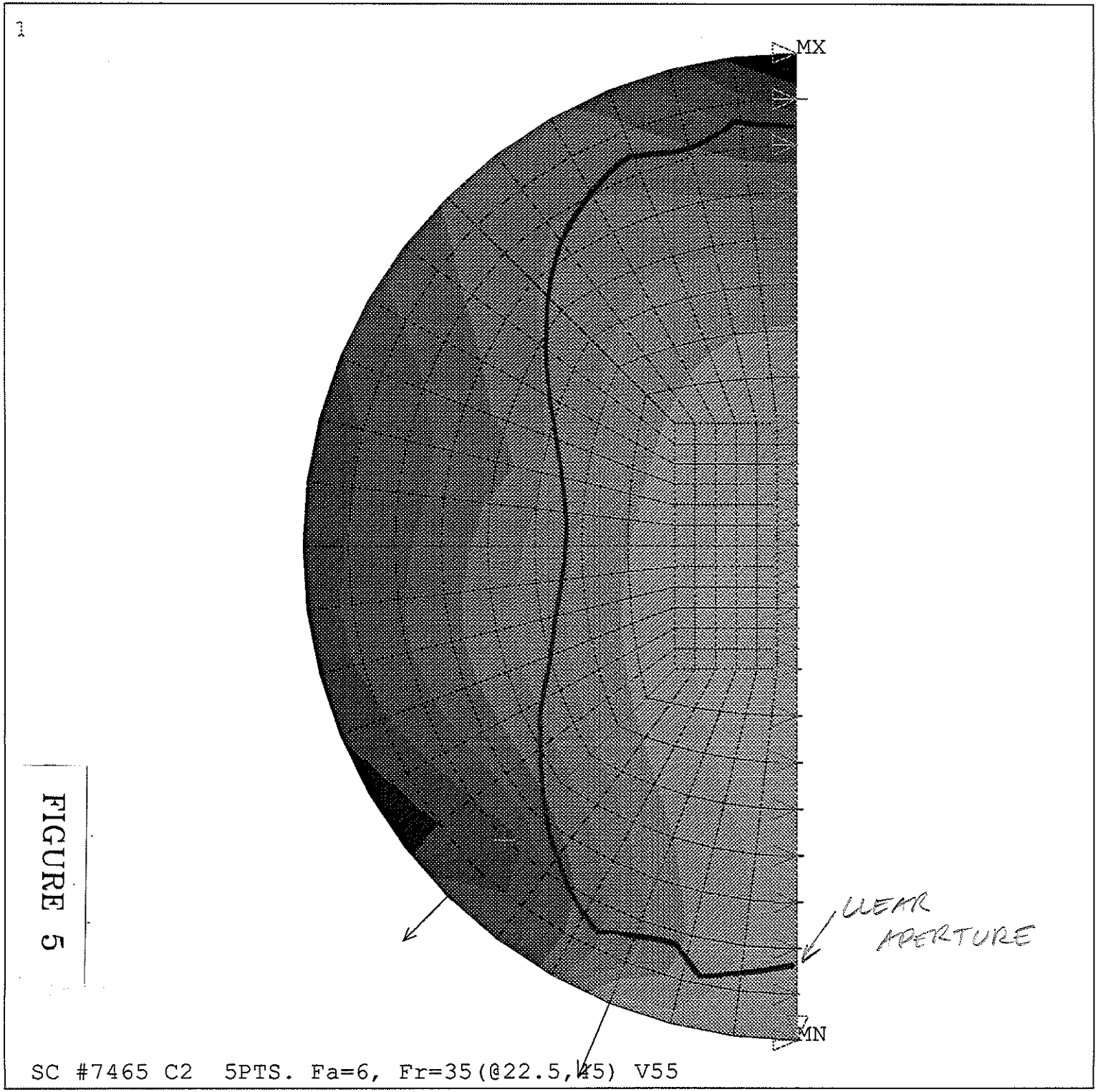
MX
MN
WEAR APERTURE
SC #7465 C2 5PTS. Fa=6, Fr=35(@22.5,45) V55
ANSYS 4.4A
AUG 18 1992
13:46:51
PLOT NO. 1
POST1 STRESS
STEP=1
ITER=1
UY
D GLOBAL
SMN =-0.686E-05
SMX =0.130E-05
TDIS
FORC
YV =-1
DIST=17.677
YF =-1.437
ZF =-8.035
VUP =-X
FACE HIDDEN
-0.686E-05
-0.595E-05
-0.504E-05
-0.414E-05
-0.323E-05
-0.232E-05
-0.142E-05
-0.510E-06
0.396E-06
0.130E-05

FIGURE 5

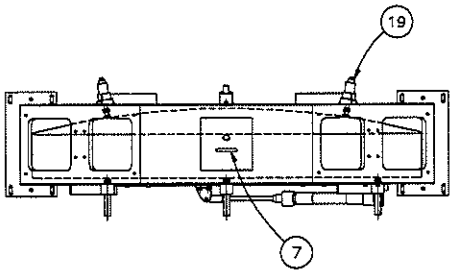

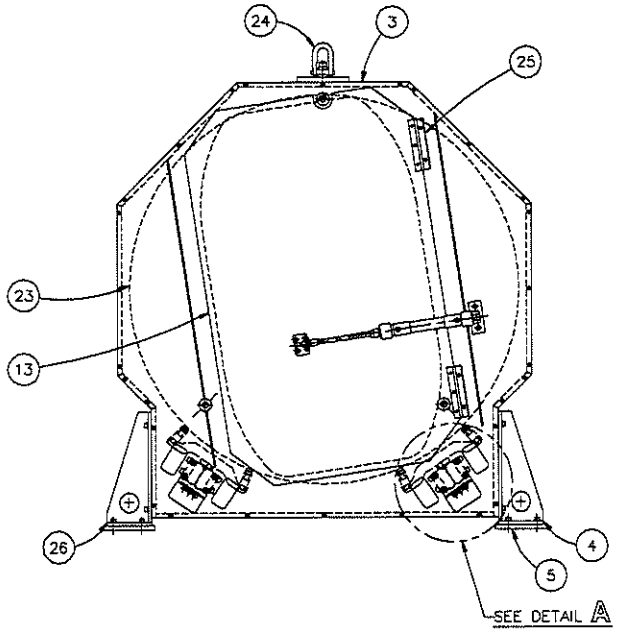

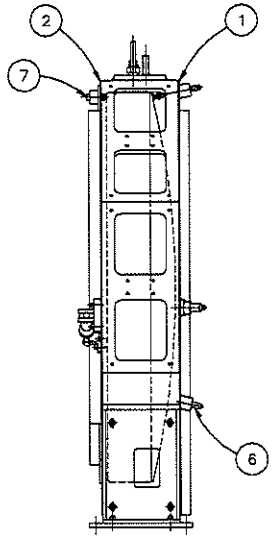

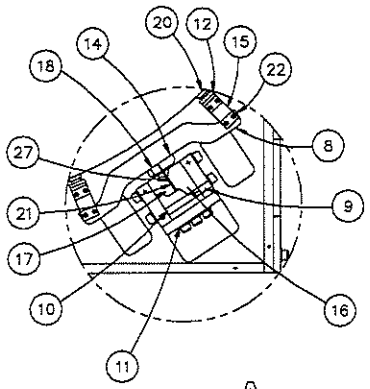

DETAIL A

SCALE 1/2
DOOR & BACK PLATE REMOVED FOR CLARITY

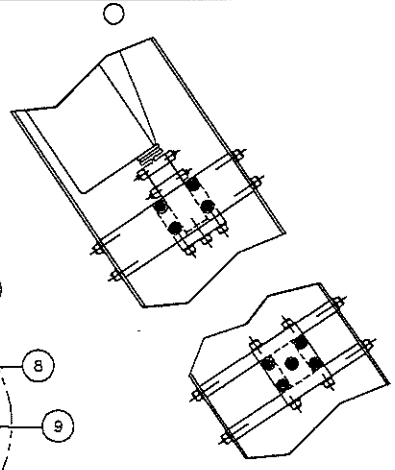

H5335-8	27	2	SPACER	SST					
H5341-2	26	1	CELL MOUNT WELD	STEEL	H5342-1	13	1	DOOR ASSY	
H5333-2	25	2	SPACER	STEEL	H5335-3	12	4	SUPPORT ARM	ST.STEEL
--	24	1	HOIST RING		H5336-2	11	2	BASE PLATE	STEEL
H0142-1	23	1	#7465 CORRECT. LENS	SILICA	H5336-3	10	4	SIDE PLATE	STEEL
H5335-4	22	4	CLAMP	ST.STEEL	H5336-4	9	4	BEAM	STEEL
H5335-8	21	2	SPRING	ST.STEEL	H5336-1	8	2	ROCKER ARM	ALUM
H5335-1	20	4	LENS CONTACT PAD	DELRIN	H5328-2	7	4	RETAINING POINT	
H5328-3	19	2	FORCE POINT		H5328-1	6	3	DEFINING POINT	
H5335-7	18	2	CLAMP	ST.STEEL	H5332-4	5	2	MOUNTING PLATE	STEEL
H5335-6	17	2	CLAMP	ALUM	H5341-1	4	2	CELL MOUNT WELD.	STEEL
H5335-5	16	2	CLAMP	ST.STEEL	H5343-1	3	1	MONISCUS CORRECT CELL WELD	
H5335-7	15	6	SPRING	ST.STEEL	H5338-1	2	1	BACK PLATE WELD.	STEEL
H5335-5	14	2	CLAMP	ALUM	H5338-1	1	1	FRONT PLATE WELD.	STEEL

1/4

REV			
A	11/7/91	CAO	UPDATE PER AS BUILT
B	11/26/91	CAO	ADDED PARTS 27 & 20

KECK/HIRES

MENISCUS CORRECTOR CELL ASSEMBLY

D.C.S. 10/1/91
C.A.O. 11/4/91

H5324.B

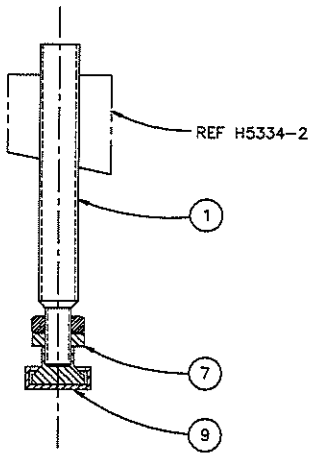

-1 DEFINING POINT

3 REQ'D – MENISCUS CORRECTOR CELL
3 REQ'D – BICONVEX CORRECTOR CELL

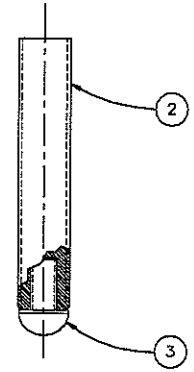

-2 RETAINING POINT

4 REQ'D – MENISCUS CORRECTOR CELL
4 REQ'D – BICONVEX CORRECTOR CELL

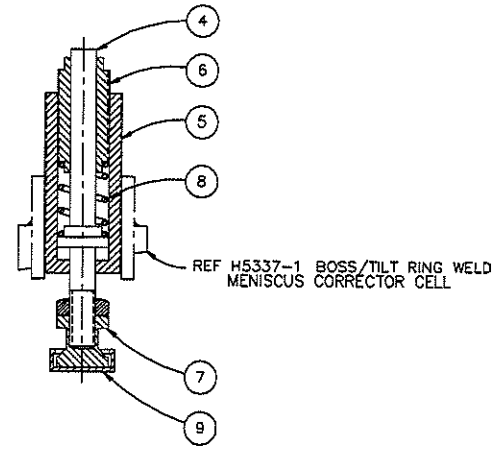

-3 FORCE POINT

2 REQ'D – MENISCUS CORRECTOR CELL
SPRING COMPRESSION = 0.542"
C DESIGN FORCE = 11.5 LBS.

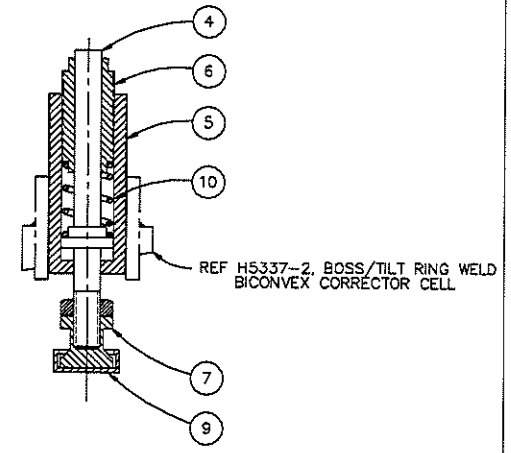

-4 FORCE POINT

2 REQ'D – BICONVEX CORRECTOR CELL
SPRING COMPRESSION = 0.540
C DESIGN FORCE = 6.0 LBS.

–	10	1	SPRING	ST. STEEL
H5334-14	9	1	CAP	TEFLON
–	8	1	SPRING	ST. STEEL
–	7	1	TOGGLE PAD	
H5334-10	6	1	TENSION ADJUSTER	SST
H5334-7	5	1	BODY	SST
H5334-6	4	1	SHAFT	SST
H5334-5	3	1	BUTTON	DELRIN
H5334-3	2	1	SHAFT	SST
H5334-1	1	1	SHAFT	SST

2/1

A	8/2/91	CAO	ADDED ITEM -4
B	7/15/92	CAO	REPLACED TEFLON TAPE W/ CAP
C	9/9/92	BCB	ADDED SPRING AND FORCE DATA

KECK/HIRES
CORRECTOR CELL
AXIAL SUPPORT DETAILS

BCB 8/1/91
CAO 8/16/91

H5328.C

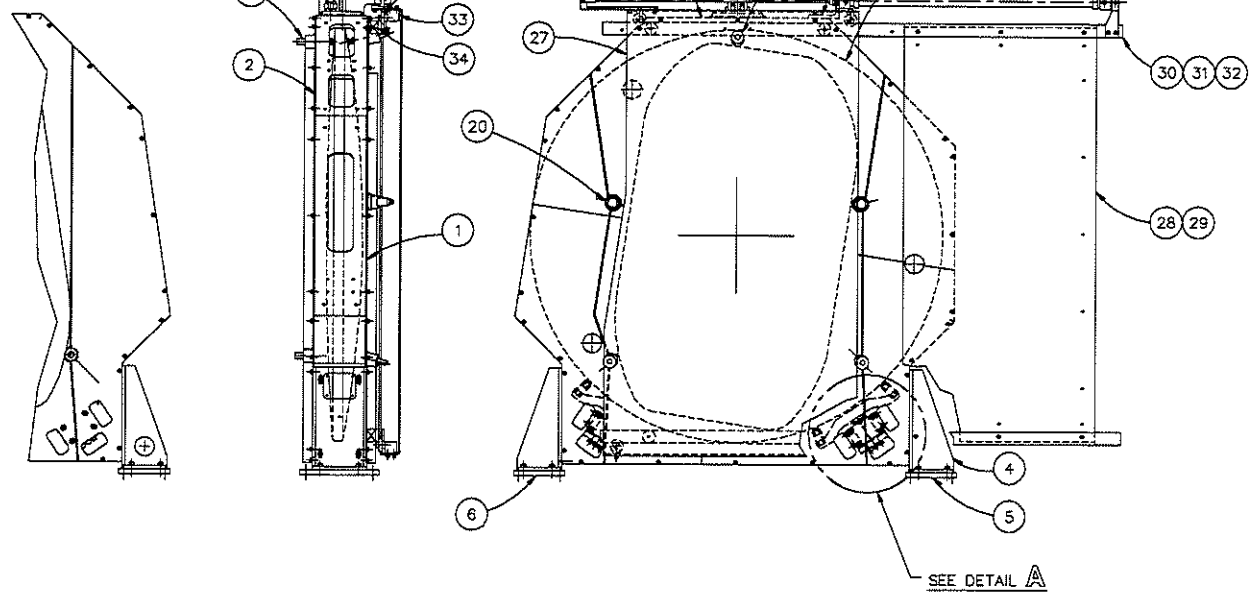

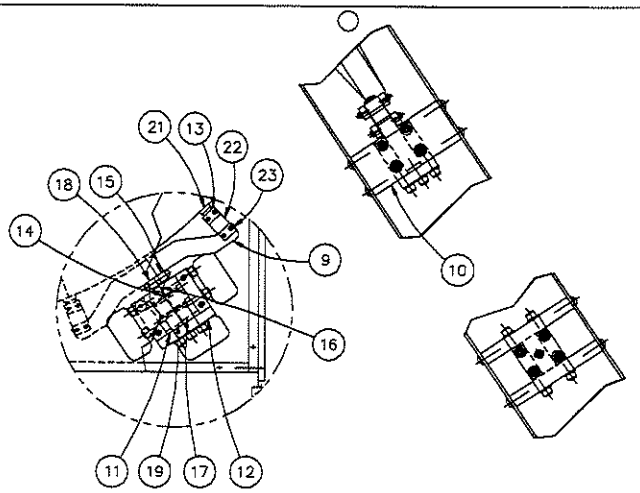

DETAIL A

SCALE 1/2

					H5328-4	20	2	FORCE POINT	
–	39	1	AIR CYLINDER		H5361-5	19	2	CLAMP	ST.STEEL
H5347-8	38	1	AIR CYLINDER SUPPORT	ALUM	H5361-4	18	2	CLAMP	ALUM
H5347-3	37	1	AIR CYLINDER SUPPORT	ALUM	H5361-3	17	2	CLAMP	ST.STEEL
H5347-4	36	1	AIR CYLINDER SUPPORT	ALUM	H5361-2	16	2	SPRING	ST.STEEL
H5347-3	35	4	WHEEL	DELRIN	H5361-1	15	2	CLAMP	ALUM
H5347-2	34	4	STANDOFF	ALUM	H5361-6	14	2	SPACER	SST
H5347-1	33	4	WHEEL MOUNT	ALUM	H5358-5	13	2	CONTACT SUPPORT	ST.STEEL
H5348-3	32	2	SPACER	ALUM	H5358-4	12	2	BASE PLATE	STEEL
H5348-2	31	2	RAIL	ALUM	H5358-3	11	4	SIDE PLATE	STEEL
H5348-1	30	2	RAIL	ALUM	H5358-2	10	4	BEAM	STEEL
H5345-2	29	2	SPACER	ALUM	H5358-1	9	2	ROCKER ARM	ALUM
H5345-1	28	1	PANEL	ALUM	H5328-2	8	4	RETAINING POINT	
H5344-1	27	1	DOOR	ALUM	H5328-1	7	3	DEFINING POINT	
H5333-2	26	2	SPACER	STEEL	H5357-3	6	1	MOUNTING PLATE	STEEL
–	25	1	HOIST RING		H5357-2	5	1	MOUNTING PLATE	STEEL
H0141-1	24	1	#7465 CORRECT. LENS	SILICA	H5364-1	4	2	CELL MOUNT WELD.	STEEL
H5335-4	23	4	CLAMP	ST.STEEL	H5368-1	3	1	BICONVEX CORRECT CELL WELD	
H5335-2	22	4	SPRING	ST.STEEL	H5366-1	2	1	BACK PLATE WELD.	STEEL
H5358-6	21	2	LENS CONTACT PAD	DELRIN	H5365-1	1	1	FRONT PLATE WELD.	STEEL

1/4

REV			
A	11/7/91	CAD	UPDATE PER AS BUILT
B	5/11/92	CAD	REVISED WITH DOOR MOD

KECK/HIRES

BICONVEX CORRECTOR CELL ASSEMBLY

S.G.S. 9/1/91

C.A.D. 10/23/91

H5349.B

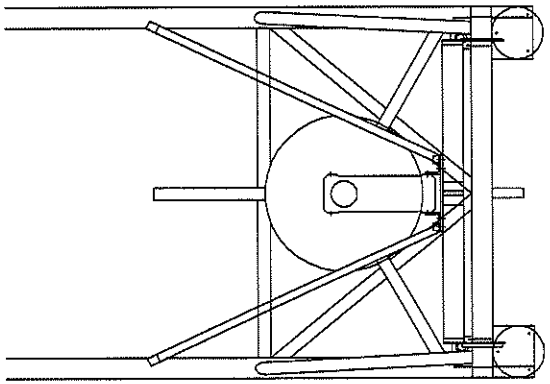

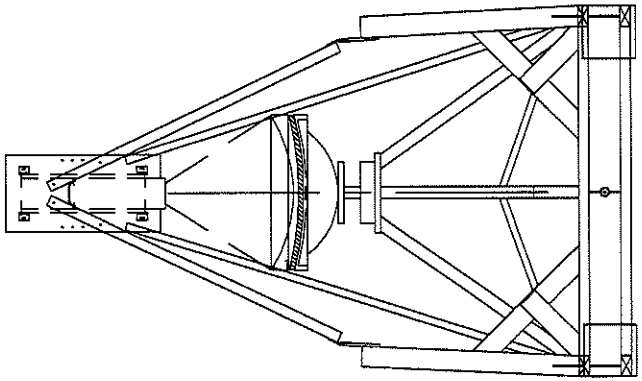

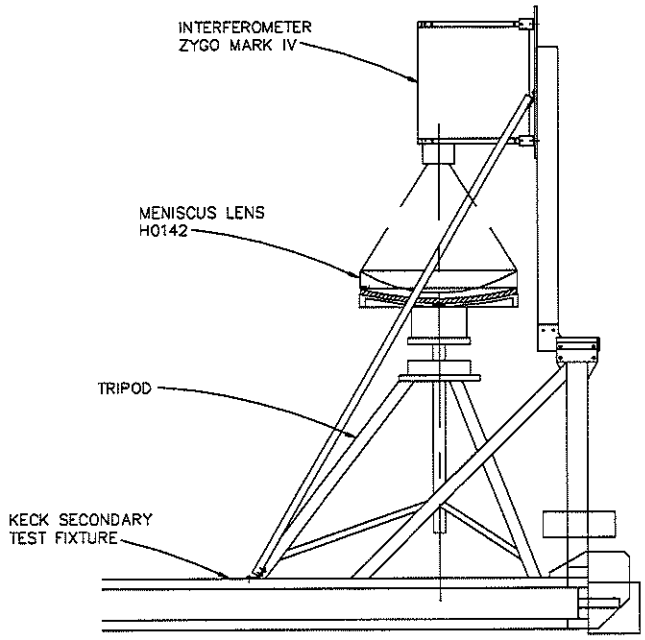

REV

.1

KECK/HIRES

MENISCUS LENS
HORIZONTAL TEST ASSY

B.C.B. 6/12/92
C.A.C. 6/24/92

H5811

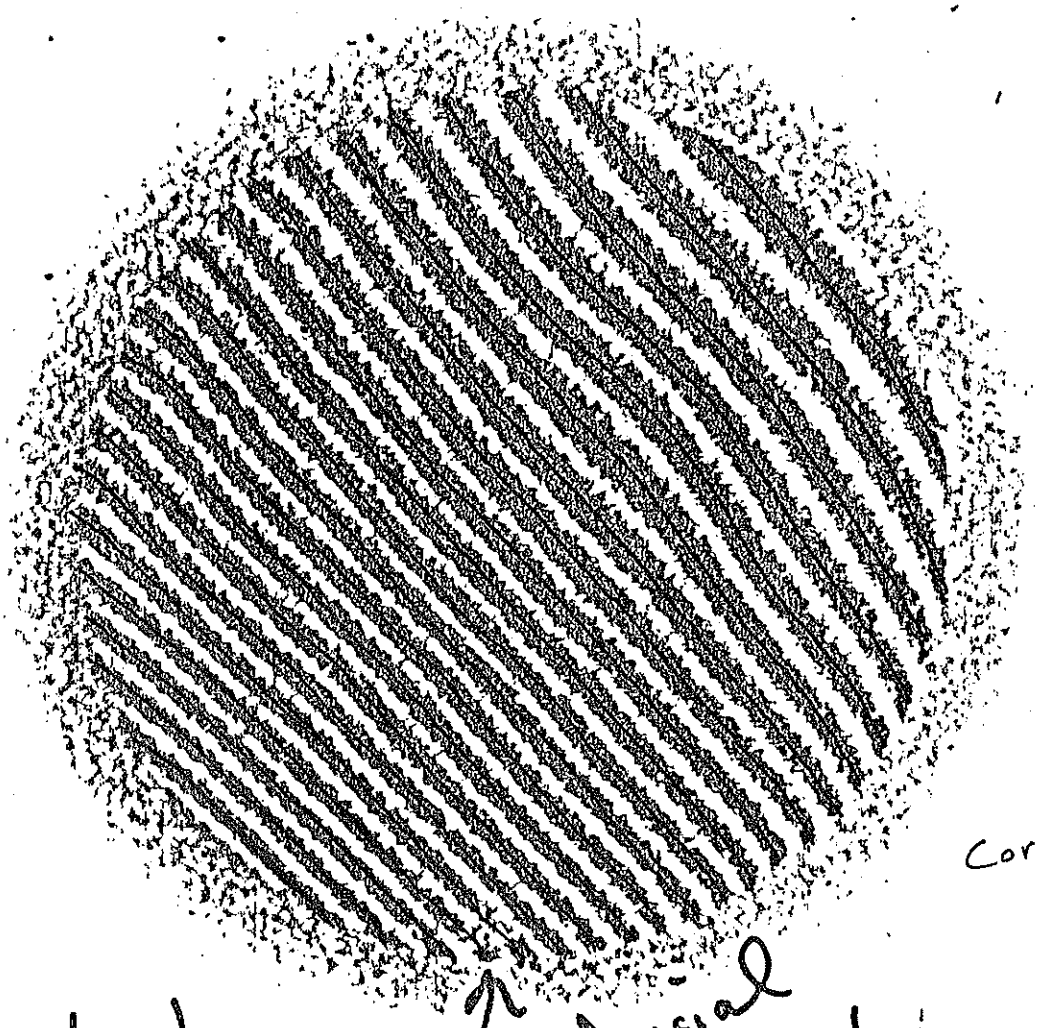
Fig. 6
Corr #1
Corrector #2
Concave
Horizontal
#1
Fiducial
Center Hole
Ele. #2 Horiz.

FIGURE 6

^WISP [Ver. 3.13] SN- 189 07-14-92

Cor 2 Horz #1 14:10:18 07-13-92
OPD data

TERM	RMS FIT	COEFFICIENTS			
TILT	0.300	3.7373	3.7744		
FOCUS	0.257	3.7337	3.7895	0.2825	
SEIDEL	0.065	3.7348	3.7800	0.2869	-0.2268
		0.6200	0.0247	-0.0042	-0.0197

	AMT	ANGLE
TILT	5.285	45.8
FOCUS	0.032	
ASTIG	1.320	55.0
COMA	0.075	-9.7
SA3	-0.118	

TERMS REMOVED: TILT FOCUS

x center	y center	radius
50.00	50.00	47.27

DATA PTS	WEDGE	PEAK	VALLEY	P-V	RMS	STREHL RATIO
6422	0.50	0.646	-0.829	1.475	0.256	0.076

FIGURE 7

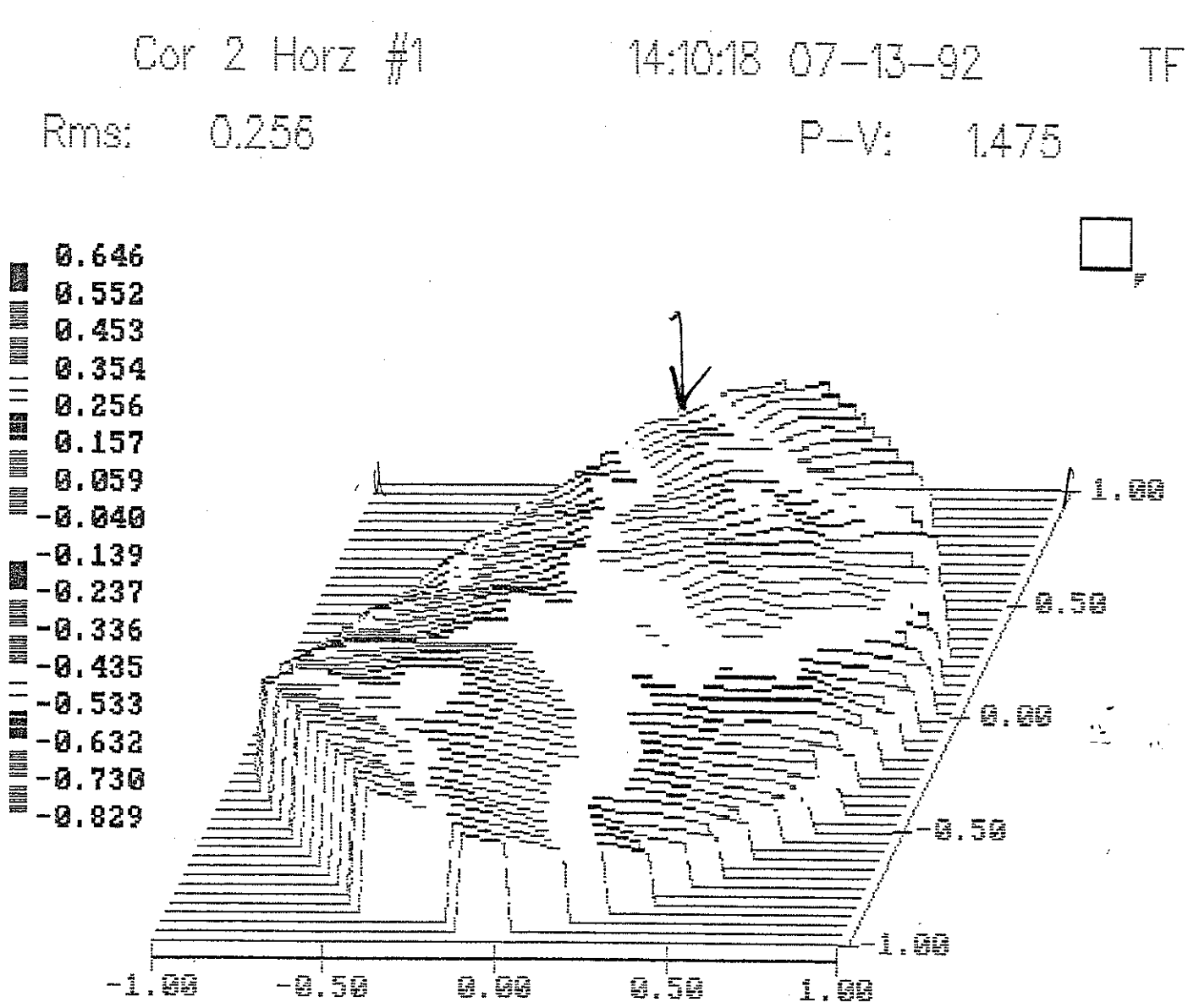
Cor 2 Horz #1
14:10:18 07-13-92
TF
Rms: 0.256
P-V: 1.475
0.646
0.552
0.453
0.354
0.256
0.157
0.059
-0.040
-0.139
-0.237
-0.336
-0.435
-0.533
-0.632
-0.730
-0.829
1.00
0.50
0.00
-0.50
-1.00
-1.00
-0.50
0.00
0.50
1.00

FIGURE 8

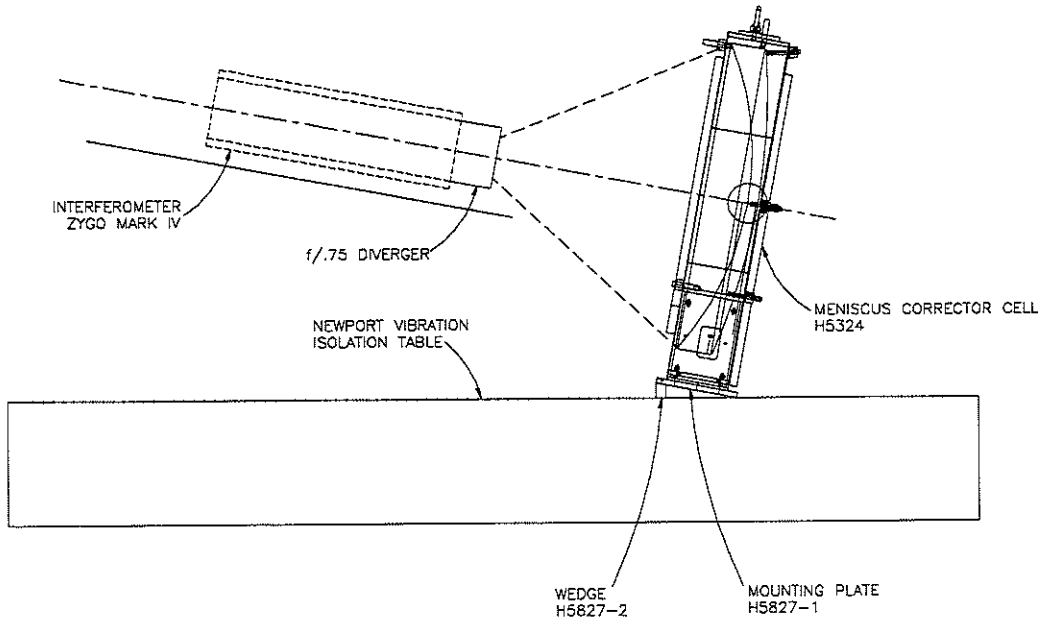

.2

REV

KECK/HIRES
MENISCUS LENS
10" TEST SET-UP

B.C.B. 8/1/92
C.A.G. 8/24/92

H5826

Corrector #2 7-11-94

10° Lean

No Tweaking / 3 pt. support

File: CR2NF#1 / No Forces

#1

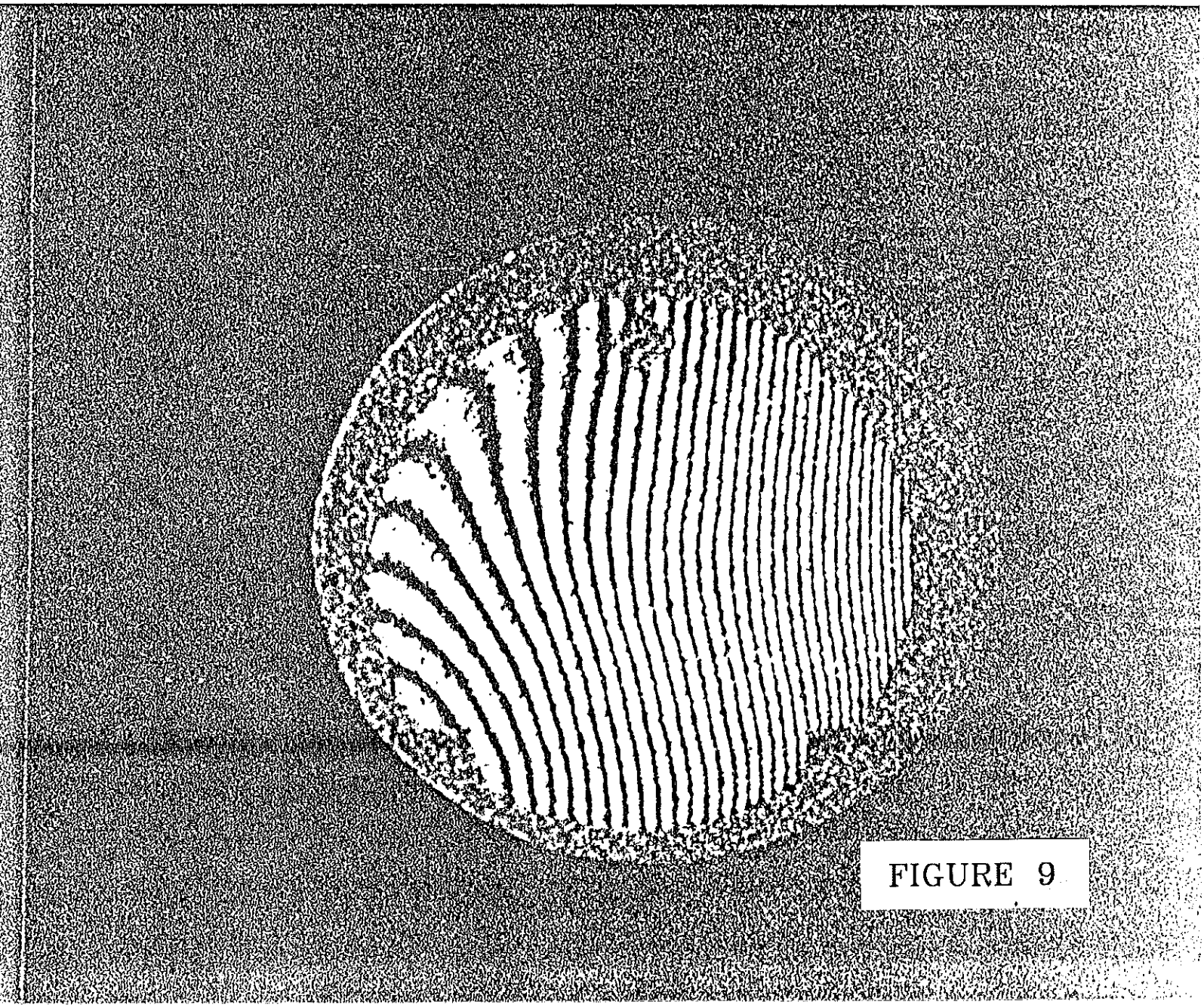

FIGURE 9

^^WISP [Ver. 3.13] SN- 189 08-02-92

Corr #2 No Forces 08:29:44 08-02-92
OPD data

TERM	RMS FIT	COEFFICIENTS			
TILT	0.696	-7.6851	-0.8952		
FOCUS	0.694	-7.6660	-0.9038	-0.1069	
SEIDEL	0.117	-7.3662	-0.9031	-0.4588	-1.9899
		0.3600	0.0152	0.0102	-0.1650

	AMT	ANGLE
TILT	7.454	187.1
FOCUS	-1.950	
ASTIG	4.044	84.9
COMA	0.055	33.9
SA3	-0.990	

TERMS REMOVED: TILT FOCUS

x center	y center	radius
52.00	50.00	47.27

DATA PTS	WEDGE	PEAK	VALLEY	P-V	RMS	STREHL RATIO
6164	0.50	1.504	-2.843	4.347	0.747	0.000

FIGURE 10

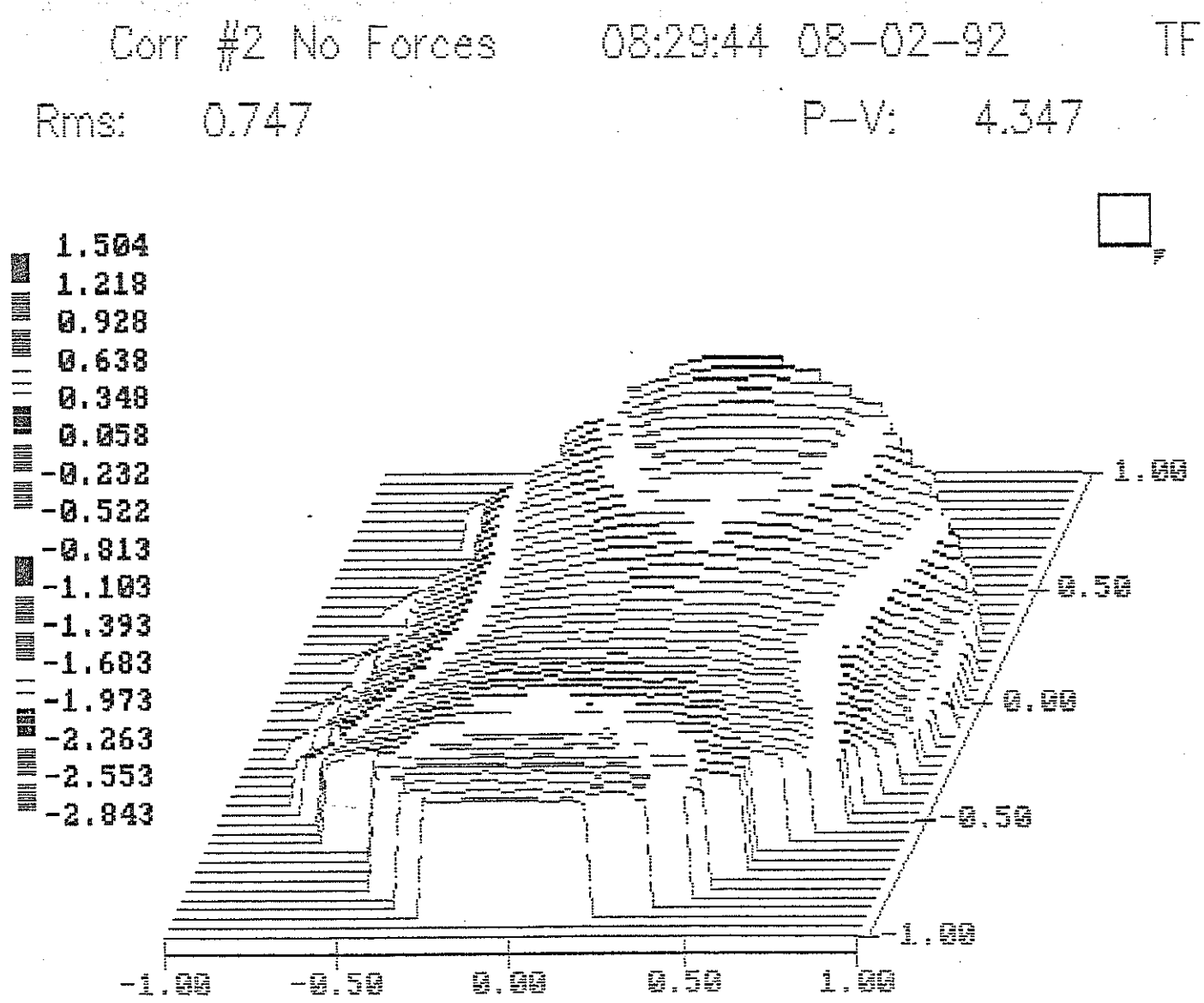
Corr #2 No Forces 08:29:44 08-02-92 TF
Rms: 0.747
P-V: 4.347
1.504
1.218
0.928
0.638
0.348
0.058
-0.232
-0.522
-0.813
-1.103
-1.393
-1.683
-1.973
-2.263
-2.553
-2.843
1.00
0.50
0.00
-0.50
-1.00
-1.00
-0.50
0.00
0.50
1.00

FIGURE 11

WISP [Ver. 3.13] SN- 189 08-02-92
Corr #2 No Forces 08:29:44 08-02-92
OPD data

TERM	RMS FIT	COEFFICIENTS			
TILT	0.657	11.0753	4.6397		
FOCUS	0.620	10.9923	4.6851	0.4158	
SEIDEL	0.092	10.7366	4.6347	0.7071	1.7015
		0.2194	-0.0298	-0.0073	0.1394

	AMT	ANGLE
TILT	11.755	23.3
FOCUS	-1.102	
ASTIG	3.431	3.7
COMA	0.092	193.8
SA3	0.801	

TERMS REMOVED: TILT FOCUS
REF SUBTRACTED: c:\wispdata\cor2h#1.opd

x center	y center	radius
51.00	50.00	46.27

DATA PTS	WEDGE	PEAK	VALLEY	P-V	RMS	STREHL RATIO
5894	-0.50	2.421	-1.331	3.752	0.629	0.000

FIGURE 12

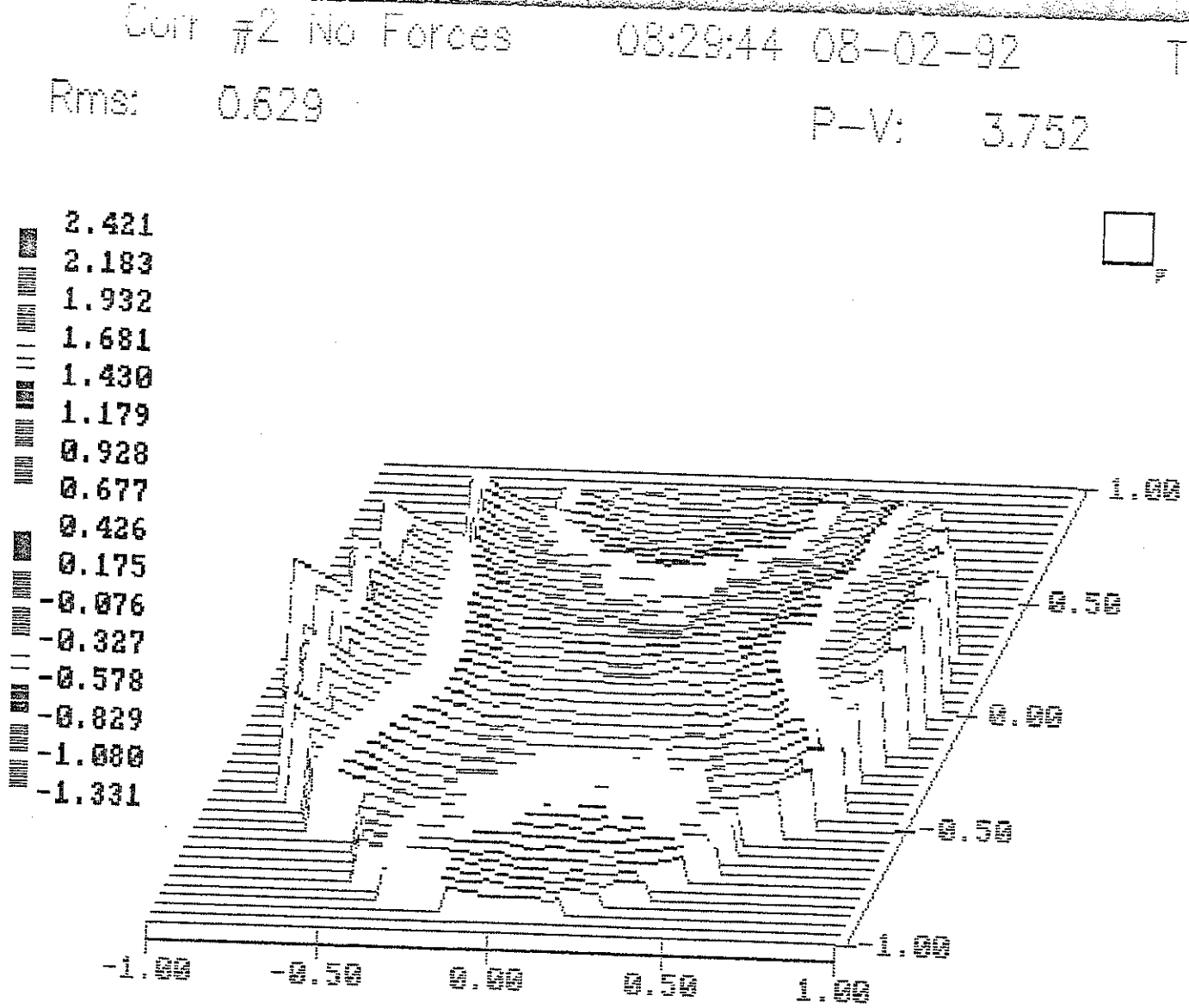
Corr #2 No Forces 08:29:44 08-02-92 TF
Rms: 0.629
P-V: 3.752
2.421
2.183
1.932
1.681
1.430
1.179
0.928
0.677
0.426
0.175
-0.076
-0.327
-0.578
-0.829
-1.080
-1.331
1.00
0.50
0.00
-0.50
-1.00
-1.00
-0.50
0.00
0.50
1.00

FIGURE 13

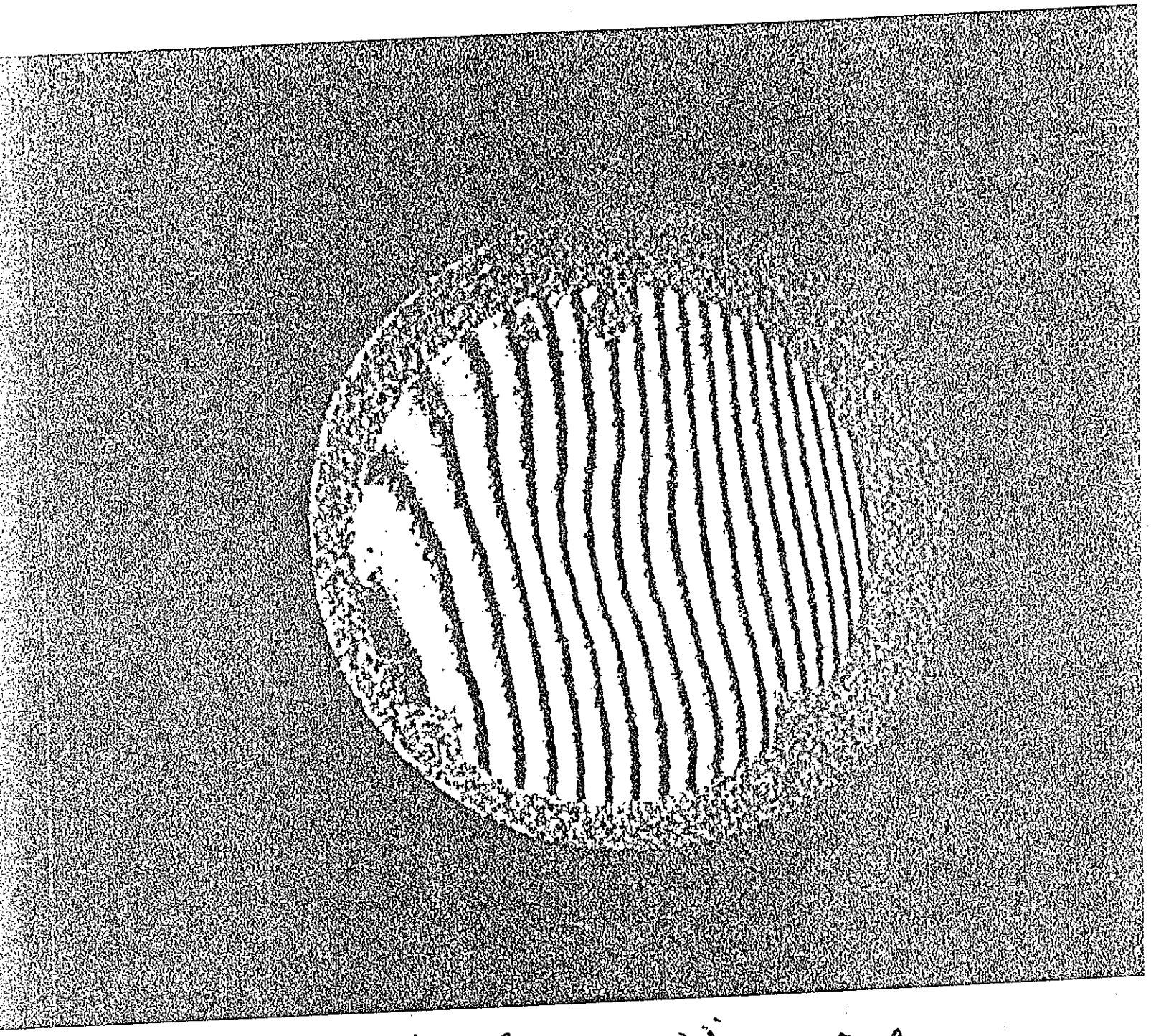

#1 Forces Applied

File: ~~CR2CFA~~ CR2CFA#1

= Corr. #2 cell Forces Applied #1

FIGURE 14

~~WISP [Ver. 3.13] SN- 189 07-18-92

Corr#2 Cell Forces 11:00:03 07-18-92
OPD data

TERM	RMS FIT	COEFFICIENTS			
TILT	0.339	-4.6416	-0.3263		
FOCUS	0.234	-4.6268	-0.3249	-0.0989	
SEIDEL	0.073	-4.5171	-0.3339	-0.2135	-0.6149
		-0.0340	0.0495	-0.0044	-0.1574

	AMT	ANGLE
TILT	4.628	184.0
FOCUS	-0.099	
ASTIG	1.232	-88.4
COMA	0.149	-5.1
SA3	-0.944	

TERMS REMOVED: TILT FOCUS

x center	y center	radius
51.00	50.00	47.10

DATA PTS	WEDGE	PEAK	VALLEY	P-V	RMS	STREHL RATIO
6213	0.50	0.509	-0.971	1.479	0.237	0.110

FIGURE 15

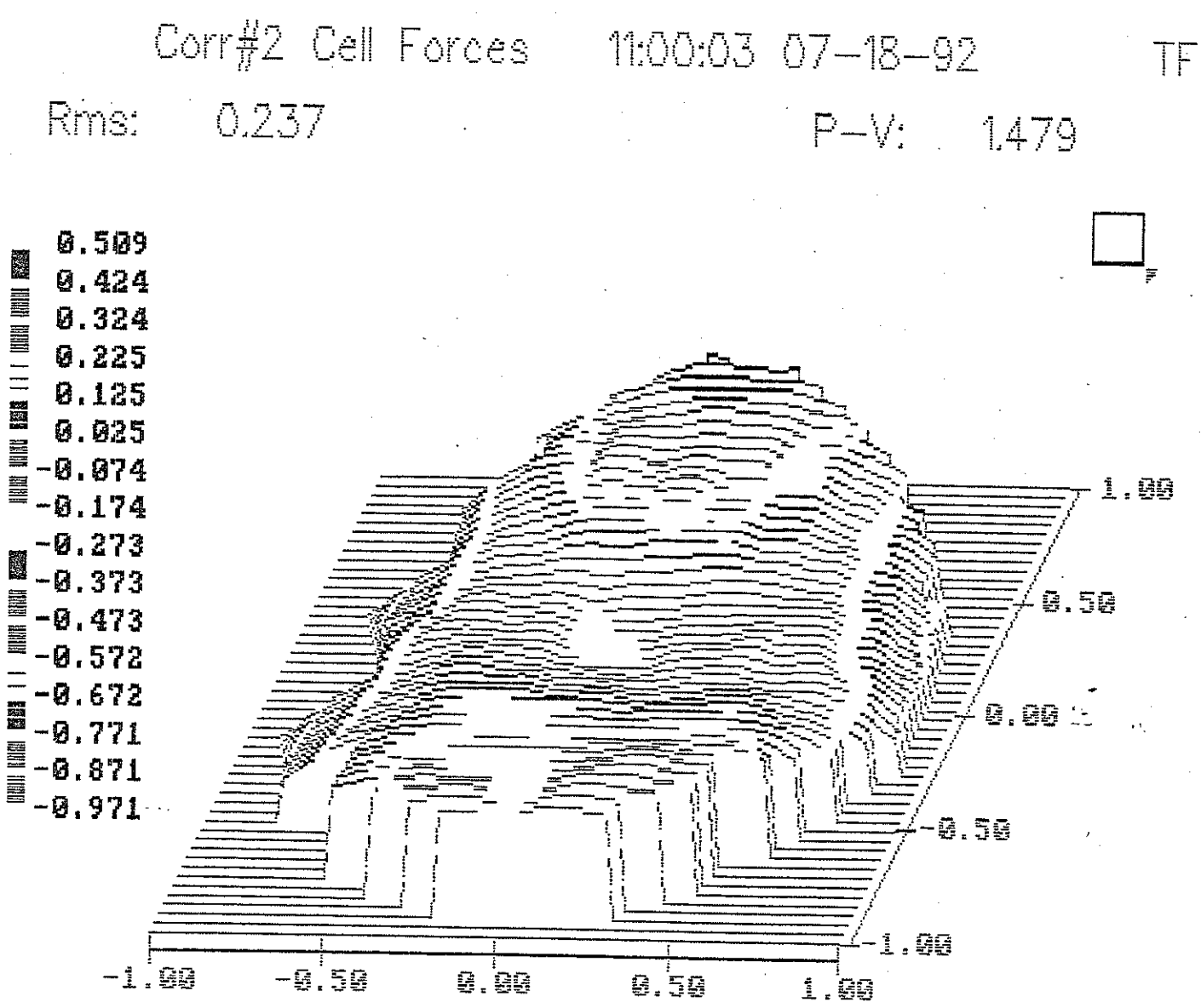
Corr#2 Cell Forces 11:00:03 07-18-92 TF
Rms: 0.237
P-V: 1.479
0.509
0.424
0.324
0.225
0.125
0.025
-0.074
-0.174
-0.273
-0.373
-0.473
-0.572
-0.672
-0.771
-0.871
-0.971
1.00
0.50
0.00
-0.50
-1.00
-1.00
-0.50
0.00
0.50
1.00

FIGURE 16

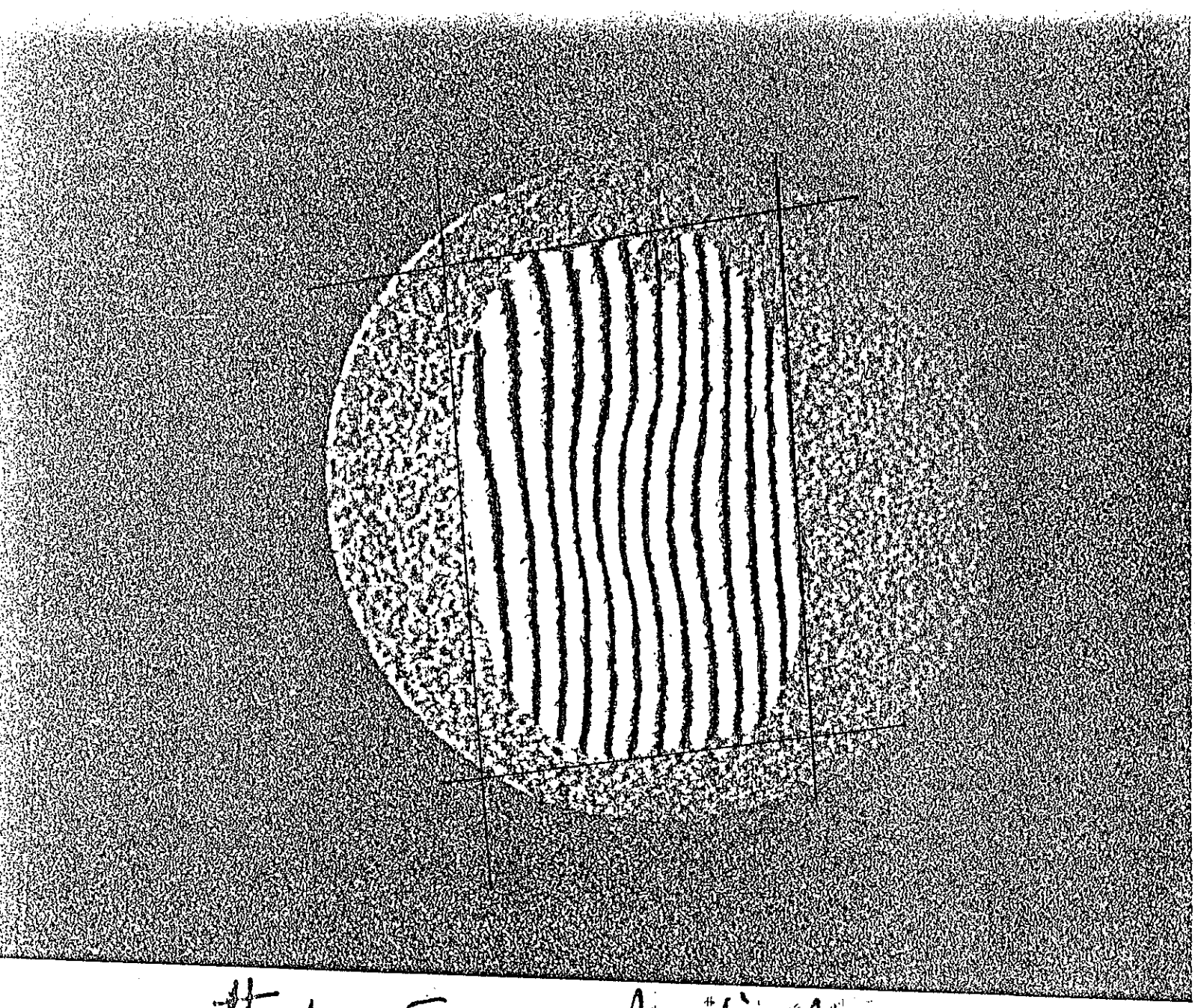

#1 Forces Applied 7-20-92
Masked C.A.
Corr. #2

File: CR2FAC1

Final 10° Lean Test
Best Representative
Forces applied.
P-V. = .65T

FIGURE 17

Corr2 Cell Forces CA 06:42:40 07-19-92
OPD data

TERM	RMS FIT	COEFFICIENTS			
TILT	0.103	-4.9845	-0.0879		
FOCUS	0.097	-4.9897	-0.0828	0.0653	
SEIDEL	0.060	-4.8561	-0.0994	-0.1466	-0.3611
		0.0887	0.1285	-0.0331	-0.1432

	AMT	ANGLE
TILT	5.113	180.4
FOCUS	0.194	
ASTIG	0.744	83.1
COMA	0.398	-14.5
SA3	-0.859	

TERMS REMOVED: TILT FOCUS

x center	y center	radius
50.00	50.00	39.81

DATA PTS	WEDGE	PEAK	VALLEY	P-V	RMS	STREHL RATIO
3096	0.50	0.222	-0.427	0.648	0.103	0.656

FIGURE 18

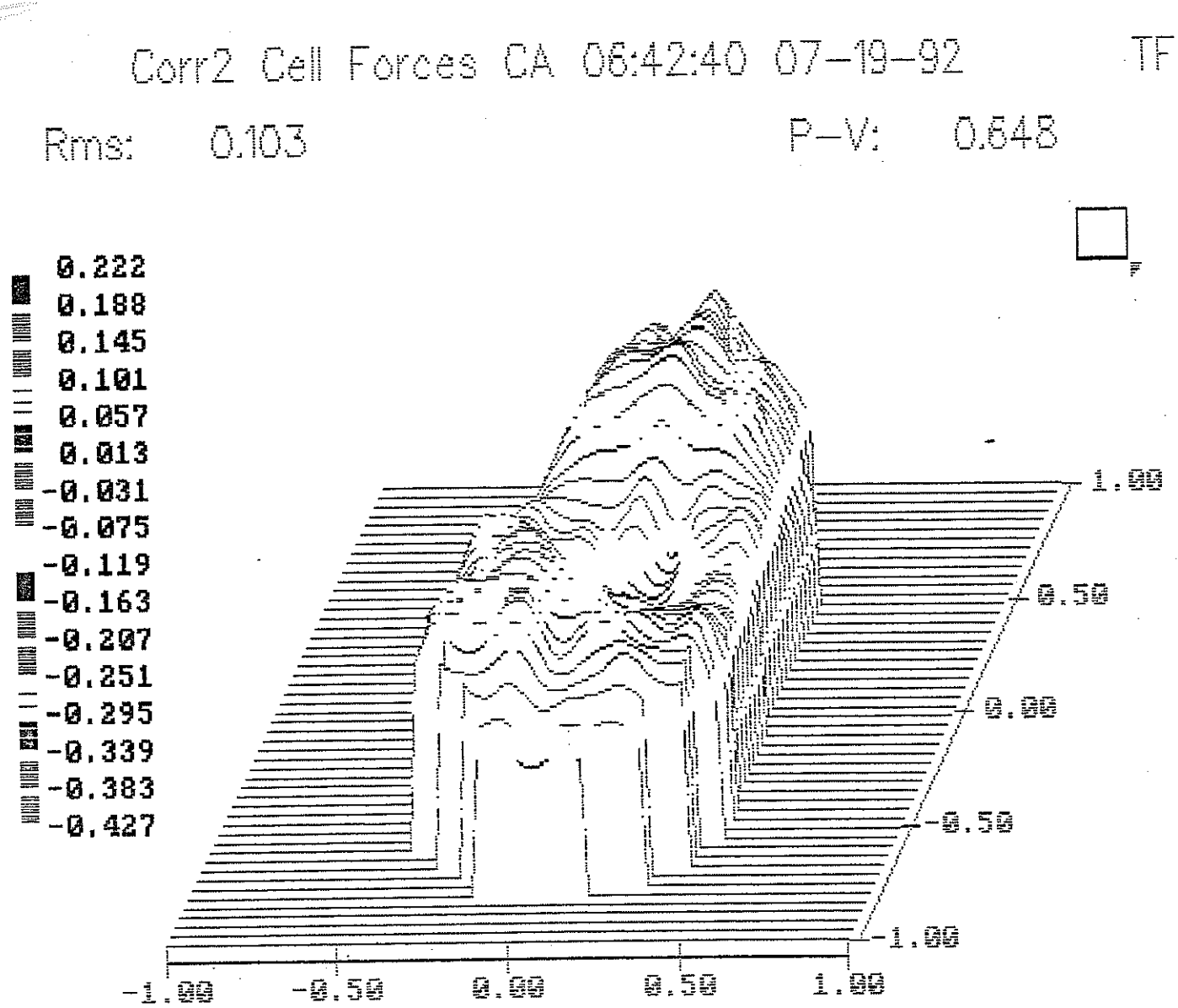
Corr2 Cell Forces CA 06:42:40 07-19-92
TF
Rms: 0.103
P-V: 0.648
0.222
0.188
0.145
0.101
0.057
0.013
-0.031
-0.075
-0.119
-0.163
-0.207
-0.251
-0.295
-0.339
-0.383
-0.427
1.00
0.50
0.00
-0.50
-1.00
-1.00
-0.50
0.00
0.50
1.00

FIGURE 19

APPENDIX A

```
/prep7
/show,x11
/title, SC #7465 C1 RAD(90/45)/5 AX. F=10.5 V54
! solid model with nodes at 60 deg.
! /home/bruce/anfiles/sc7465/c1/v54/geomod
! for concave-concave r1 is +, r2 is -
! for convex-convex r1 is -, r2 is +
! for concave-convex r1 is +, r2 is +
! for plano- let r -> very large
! d is diameter of part
! t is distance between surfaces at the center
!
! --- input optic parameters ---
!
r1=28.5
r2=62.6
d=30.3
t=1
yfor=10.5
!
! --- input geometric model parameters ---
!
! tdiv is angular (theta) divisions
! thdv is thickness divisions
! rdiv is radial divisions
! thet is angle between vertical and simple support:
!
tdiv=6
thdv=4
rdiv=8
thet=45
!
! --- material type and constants ---
!
!  optic material is fused silica
!
ex=10.58792e6
nu=.17
dens=.0796
!
! --- start model input ---
kan,0
!  local coord systems for radii of f & r curves
local,11,2,0,r1,0,0,0,0
local,12,2,0,((-t)+r2),0,0,0,0
csys,11
k,,r1,-90
k,,abs(r1),((-45)*r1)/(abs(r1))
kmov,2,11,abs(r1),999,0,0,d/2,999,999
l,1,2
csys,12
k,,r2,-90
k,,abs(r2),-45*r2/abs(r2)
kmov,4,12,abs(r2),999,0,0,d/2,999,999
l,3,4
l,2,4
l,3,1
csys
kgen,2,1,,,d/8,d/8
kgen,2,3,,,d/8,-d/8
l,5,6
lint,5,1
,2,6
ldel,5,,,1
,9,,,1
local,13,1,0,0,0,0,0,-90
```

```
lsrs,,3
lsas,,6,8
lgen,2,all,,,0,90
lgen,2,3,,,0,45
l,2,11
,4,12
,12,6
,11,5
lsal
kgen,2,7,,,0,45
kmov,13,11,r1,999,999,13,(d*1.414)/8,45,999
csys,11
l,7,13
,9,13
,1,9
,13,11
csys,13
kgen,2,8,,,0,45
kmov,14,12,abs(r2),999,999,13,(d*1.414)/8,45,999
csys,12
l,8,14
,14,10
,10,3
,14,12
csys
l,13,14
!   stop to check geometry
!fini
!/eof
!
V,      3,      8,     14,     10,      1,      7,     13,      9
V,      8,      4,     12,     14,      7,      2,     11,     13
V,     10,     14,     12,      6,      9,     13,     11,      5
!  lines in theta direction
LSRS,LINE,          2
LSAS,LINE,          1
LSAS,LINE,         17
LSAS,LINE,         18
LSAS,LINE,         15
LSAS,LINE,         16
LSAS,LINE,         19
LSAS,LINE,         23
LSAS,LINE,         22
LSAS,LINE,         21
LSAS,LINE,         13
LSAS,LINE,         14
ldvs,all,,tdiv
!  ldvs = 3 creates nodes at 30 deg. intervals
lsal
!  lines in thickness
LSRS,LINE,          4
LSAS,LINE,          6
LSAS,LINE,         25
LSAS,LINE,          9
LSAS,LINE,          5
LSAS,LINE,         12
LSAS,LINE,          3
ldvs,all,,thdv
!  ldvs = 4 creates 4 layers of elements in depth
lsal
!  lines in radial
LSRS,LINE,         10
LSAS,LINE,         11
LSAS,LINE,         20
LSAS,LINE,         24
LSAS,LINE,          7
```

```
LSAS,LINE,          8
ldvs,all,,rdiv
!  ldvs = 6 creates 6 layers in the radial direction
lsal
vsym,1,all
numm,kpoi
et,1,45
elsi,,1,2
vmes,all
csys
wsort,x
nsel,z,0
d,all,uz
nall
mp,ex,1,ex
mp,nuxy,1,nu
mp,dens,1,dens
vsum
*get,vl,gsum,volu
!  find and enter model volume "vl"
*get,yct,gsum,yc
!  find and enter y centroid "yct"
wt=vl*dens
!
arse,,9,13,4
lsrs,,3
lsum
*get,ll,gsum,leng
!   line length "ll" from lsum
!
!          ----  Macro to model simple support ----
*create,thta
!
csys,13
nsel,x,d/2
nrse,y,22,46
nuse,y,24,44
nrse,z,0.8,1.8
nrot,all
d,all,ux
nall
*end
!
!
!          ----  Macro for front forcing points using nodes ----
*create,forc
!
csys,12
nsel,x,(r2-.1),(r2+.1)
csys,13
nrse,x,9,10
nrse,y,88,92
csys
f,all,fy,yfor
nall
*end
!
!          ----  Macro for front def. points using nodes ----
*create,fdef
csys,12
nsel,x,(r2-.1),(r2+.1)
csys,13
nrse,x,12,13
nrse,y,44,46
csys
d,all,uy
```

```
nlis
nall
!
csys,12
nsel,x,(r2-.1),(r2+.1)
csys,13
nrse,x,d/2
nrse,y,180
csys
d,all,uy
nall
*end
!
!
!  choose the support options
!    radial supports:
*use,thta
!    axial supports:
*use,fdef
*use,forc
!
!  --- define gravity vector by load case: ---
!
! --- loadcase gravity at 10.3 degrees
acel,-0.98,0.18
!
lwri,1
!
yfor=0
*use,forc
/title, F=0 C1 V54
lwri,2
!
yfor=11.5
*use,forc
/title, F=11.5 C1 V54
lwri,3
!
!
/pbc,tdis,1
/view,1,-.5,-1,-1
/vup,1,-x
nplo
!
afwr
fini
```

APPENDIX B

```
/prep7
/title, SC #7465 C2  5PTS. Fa=6, Fr=35(@22.5,45) V55
! solid model with nodes at 60 deg.
! /export/ansysdat/lensmod/sc7465/c2/v55
! for concave-concave r1 is +, r2 is -
! for convex-convex r1 is -, r2 is +
! for concave-convex r1 is +, r2 is +
! for plano- let r -> very large
! d is diameter of part
! t is distance between surfaces at the center
!
! --- input optic parameters ---
!
r1=-218.86
r2=87.11
d=32.14
t=2.874
!
! --- input geometric model parameters ---
!
! tdiv is angular (theta) divisions
! thdv is thickness divisions
! rdiv is radial divisions
! thet is angle between vertical and simple support:
!
tdiv=6
thdv=4
rdiv=8
thet=45
!   front face force value
yfor=6
!   radial force value
rfor=-35
!
! --- material type and constants ---
!
!  optic material is fused silica
!
ex=10.58792e6
nu=.17
dens=.0796
!
! --- start model input ---
kan,0
!  local coord systems for radii of f & r curves
local,11,2,0,r1,0,0,0,0
local,12,2,0,((-t)+r2),0,0,0,0
csys,11
k,,r1,-90
k,,abs(r1),((-45)*r1)/(abs(r1))
kmov,2,11,abs(r1),999,0,0,d/2,999,999
l,1,2
csys,12
k,,r2,-90
k,,abs(r2),-45*r2/abs(r2)
kmov,4,12,abs(r2),999,0,0,d/2,999,999
l,3,4
l,2,4
l,3,1
csys
kgen,2,1,,,d/8,d/8
kgen,2,3,,,d/8,-d/8
l,5,6
lint,5,1
,2,6
ldel,5,,,1
```

```
,9,,,1
local,13,1,0,0,0,0,0,-90
lsrs,,3
lsas,,6,8
lgen,2,all,,,0,90
lgen,2,3,,,0,45
l,2,11
,4,12
,12,6
,11,5
lsal
kgen,2,7,,,0,45
kmov,13,11,r1,999,999,13,(d*1.414)/8,45,999
csys,11
l,7,13
,9,13
,1,9
,13,11
csys,13
kgen,2,8,,,0,45
kmov,14,12,abs(r2),999,999,13,(d*1.414)/8,45,999
csys,12
l,8,14
,14,10
,10,3
,14,12
csys
l,13,14
!   stop to check geometry
!fini
!/eof
!
V,      3,      8,     14,     10,      1,      7,     13,      9
V,      8,      4,     12,     14,      7,      2,     11,     13
V,     10,     14,     12,      6,      9,     13,     11,      5
!  lines in theta direction
LSRS,LINE,          2
LSAS,LINE,          1
LSAS,LINE,         17
LSAS,LINE,         18
LSAS,LINE,         15
LSAS,LINE,         16
LSAS,LINE,         19
LSAS,LINE,         23
LSAS,LINE,         22
LSAS,LINE,         21
LSAS,LINE,         13
LSAS,LINE,         14
ldvs,all,,tdiv
!  ldvs = 3 creates nodes at 30 deg. intervals
lsal
!  lines in thickness
LSRS,LINE,          4
LSAS,LINE,          6
LSAS,LINE,         25
LSAS,LINE,          9
LSAS,LINE,          5
LSAS,LINE,         12
LSAS,LINE,          3
ldvs,all,,thdv
!  ldvs = 4 creates 4 layers of elements in depth
lsal
!  lines in radial
LSRS,LINE,         10
LSAS,LINE,         11
LSAS,LINE,         20
```

```
LSAS,LINE,          24
LSAS,LINE,           7
LSAS,LINE,           8
!ldvs,all,,rdiv,.25
ldvs,all,,rdiv
!  ldvs = 6 creates 6 layers in the radial direction
!  rdiv,.3 creates varying ele. sizes
lsal
vsym,1,all
!
! check geometry
/view,1,-.5,-1,-1
/vup,1,-x
lplo
!
numm,kpoi
et,1,45
elsi,,1,2
vmes,all
csys
wsort,x
nsel,z,0
d,all,uz
nall
mp,ex,1,ex
mp,nuxy,1,nu
mp,dens,1,dens
vsum
*get,vl,gsum,volu
!  find and enter model volume "vl"
*get,yct,gsum,yc
!  find and enter y centroid "yct"
wt=vl*dens
!
arse,,9,13,4
lsrs,,3
lsum
*get,ll,gsum,leng
!   line length "ll" from lsum
!
!
!          ----  Macro to model radial support forces ----
*create,thta
!
csys,13
nsel,x,d/2
nrse,y,22,46
nuse,y,24,44
nrse,z,-1,-1.2
nrot,all
f,all,fx,rfor
nall
!   check reaction at bottom
nsel,x,d/2
nrse,y,0
nrse,z,-1,-1.2
csys,0
d,all,ux
*end
!
!
!          ----  Macro for back def. points using nodes ----
*create,fdef
!
csys,12
nsel,x,(r2-.1),(r2+.1)
```

```
csys,13
nrse,y,180
nrse,x,14,15
csys,0
d,all,uy
nall
csys,12
nsel,x,(r2-.1),(r2+.1)
csys,13
nrse,x,13,14
nrse,y,44,46
csys,0
d,all,uy
nall
*end
!
!          ----  Macro for front forcing points ----
*create,forc
!
csys,12
nsel,x,(r2+.1),(r2-.1)
csys,13
nrse,y,104,106
nrse,x,9.5,10.5
csys
f,all,fy,yfor
nall
*end
!
!  choose the support options
!    radial supports:
*use,thta
!    axial supports:
*use,fdef
*use,forc
!
!  --- define gravity vector by load case: ---
!
! --- loadcase gravity at 10.3 degrees
acel,-0.98,0.18
!
!
!lwri,1
!
!yfor=0
!*use,forc
!/title, F=0 C2 V53
!lwri,2
!
/pbc,all,1
/view,1,-.5,-1,-1
/vup,1,-x
nplo
afwr
fini
/inp,27
```